

SCIP IV – Technical Description

Compiled by Hans-Urs Zwicky

DRAFT AS A BASIS FOR DISCUSSION

Studsvik Report

Public



Compiled by Hans-Urs Zwicky

SCIP IV – Technical Description

Abstract

SCIP IV is planned to be another five-year project with an overall budget in the order of 14 M€ (SCIP III fee +10 %), starting in July 2019. It will be organised in a similar way as SCIP III. The present report describes potential Tasks and Subtasks of SCIP IV as a basis for discussions within potential participants' organisations.

In total, 19 Subtasks are described in the present proposal. Eight Subtasks within Task 1 aim at studying fuel and cladding performance issues related to interim storage. The seven Subtasks described under Task 2 represent a continuation and extension of work performed in SCIP III to investigate LOCA issues. Even Task 3 is a continuation and extension of work performed in SCIP III related to PCI. As in SCIP III, modelling efforts supporting planning and interpretation of experiments in Tasks 1 – 3 will be concentrated in a dedicated Task. Performing all work would exceed by far the SCIP IV budget. Therefore, the interaction with potential participants is expected to provide a prioritisation that will allow defining the final scope of work within the disposable resources.

Based on the results of the prioritisation exercise, the present report will be revised and transformed into a technical description of SCIP IV, which will form the basis for potential participants to take the decision for joining the new project.

Reviewed by



Pär Beccau

Date

Approved by



Mikael Karlsson

Date

6/3-18

Table of contents

	Page
Summary	1
1 Introduction	10
2 Technical description	17
2.1 Task 1 Back end	17
2.1.1 Subtask 1.1 – Cladding creep and creep failure limits in dry storage	17
2.1.2 Subtask 1.2 – In-storage annealing: creep acceleration and ductility change	21
2.1.3 Subtask 1.3 – Creep of fuel rods under simulated dry storage conditions	23
2.1.4 Subtask 1.4 – Special fuel rods	26
2.1.5 Subtask 1.5 – Hydride reorientation	29
2.1.6 Subtask 1.6 – Delayed hydride failure during interim storage	31
2.1.7 Subtask 1.7 – Spent fuel rods in transport and handling operations and in accident scenarios	36
2.1.8 Subtask 1.8 – Failed fuel	40
2.2 Task 2 Loss-of-coolant accidents	42
2.2.1 Subtask 2.1 – Microstructure related to fuel fragmentation	42
2.2.2 Subtask 2.2 – Fuel fragmentation, relocation and dispersal in non-standard fuel	43
2.2.3 Subtask 2.3 – Separate effects tests	53
2.2.4 Subtask 2.4 – Fuel and cladding oxidation in LOCA	55
2.2.5 Subtask 2.5 – Spent fuel pool LOCA	58
2.2.6 Subtask 2.6 – Post LOCA seismic loads	59
2.2.7 Subtask 2.7 – Transient fission gas release and axial gas communication	62
2.3 Task 3 – Pellet-cladding interaction	65
2.3.1 Subtask 3.1 – Data for modelling	65
2.3.2 Subtask 3.2 – Chemistry	67
2.3.3 Subtask 3.3 – Microstructure and microchemistry	69
2.3.4 Subtask 3.4 – Operational parameters	71
2.4 Task 4 – Modelling	72
2.4.1 Background	72
2.4.2 Modelling in SCIP IV	73
3 Conclusions	76
4 References	77
Abbreviations, Acronyms	88

Tables

Table 1	Preliminary test matrix for creep testing	20
Table 2	Proposed test matrix for annealing and creep testing of one test material	23
Table 3	Preliminary test matrix for heat treatment under internal pressure	26
Table 4	Preliminary test matrix for potentially weakened fuel rods	29
Table 5	Proposed schedule for hydride reorientation tests	31
Table 6	Values of the critical parameters for DHC, as observed in out-of pile tests observed in previous studies	32
Table 7	Proposed test matrix	35
Table 8	Preliminary test matrix for fuel rods in transport and storage under normal and accident conditions	40
Table 9	Example of test matrix to generate SCC data	66

Figures

Figure 1	Old (left) and new (right) integral LOCA test device	12
Figure 2	Comparison of gamma scan and profilometry results from a LOCA tested rodlet	13
Figure 3	The role of SCIP interacting with industry partners and authorities	16
Figure 4	Schematic representation of strain/time behaviour under creep conditions	17
Figure 5	Simulation of thermal creep during vacuum drying	19
Figure 6	Schematic view of creep furnace and laser measurement equipment	19
Figure 7	Example of creep test curves, showing strain as a function of time	20
Figure 8	A simple schematic illustration of a possible system for creep testing of fuel rod specimens	25
Figure 9	Threshold stress intensity factor as a function of temperature for unirradiated Zircaloy-4 fuel cladding	32
Figure 10	Schematics of PLT specimen (left) and fixture (right)	34
Figure 11	A typical diagram from a PLT test at 227 °C, where load and crack length are plotted versus time	34
Figure 12	The 4-point bending machine in the hot cell (left) and measured force vs. displacement curve for an unirradiated verification specimen (right)	38
Figure 13	Electron probe microanalysis, plutonium distribution in as-fabricated MIMAS MOX fuel pellet; UO ₂ powder from AUC (left) and ADU (right) process [58]	46

Figure 14	Optical micrograph of Pu rich agglomerates in MIMAS AUC MOX, burnup 55 MWd/kgHM [59]	47
Figure 15	Fractography of agglomerate after 3 annual cycles of irradiation [59]	48
Figure 16	Furnace used for fuel heating tests installed in hot cell	49
Figure 17	Plot of furnace and sample temperature versus time, recorded in a typical fuel heating test	50
Figure 18	Front view of the LOCA apparatus showing the main parts	52
Figure 19	Axial temperature profile of the IR furnace in the new LOCA rig at 1200 °C	52
Figure 20	Modified heating test device for measurements of transient fission gas	65
Figure 21	Effect of hoop stress on time to failure in closed tube tests with an iodine atmosphere [95]	66
Figure 22	Preparation of TEM sample from mandrel test specimen at Studsvik by means of TEM-FIB [97]	70
Figure 23	Iodine distribution in the region of a crack tip in a mandrel test sample measured with TEM-EDX (left) and nanoSIMS (right) [97]	70

Summary

The Studsvik Cladding Integrity Project, SCIP, was launched in 2004. It was a 5 year OECD/NEA Joint Project operated by Studsvik with about 30 participating organisations, including regulatory bodies, research institutions, utilities and fuel suppliers from 13 different countries. SCIP aimed at studying basic phenomena of fuel rod failures driven by pellet-cladding mechanical interaction, thus contributing to a better understanding of fundamental failure mechanisms. Pellet cladding mechanical interaction, primarily as a function of burnup, was studied in a number of ramp tests. Key parameters important for hydrogen induced failures, in particular delayed hydride cracking and failures due to embrittlement of the cladding as a consequence of hydriding, are now much better understood and could in many cases be quantified. Concerning failures caused by stress corrosion cracking from the inside of the fuel rod (“classical” pellet-cladding interaction, PCI), equipment simulating in-core conditions was significantly improved.

Studies on pellet-related parameters, not considered in SCIP, were in the focus of SCIP II, the five year continuation of the program. The four Tasks of SCIP II dealt with a review of old ramp test results, with pellet-cladding mechanical interaction, with chemically assisted stress corrosion cracking (pellet-cladding interaction, PCI) and, as a carry-over and continuation of work performed in SCIP, with hydrogen-induced failures. Performance of advanced fuel types with additives or dopants and large grains was assessed in comparison with standard fuel by means of advanced examination techniques.

The SCIP II Program Review Group followed up a LOCA test program, performed by Studsvik on behalf of the U.S.NRC. Single-rod integral LOCA tests were performed, basically following the same procedures as applied by the Argonne National Laboratory in earlier campaigns. Significant fuel fragmentation, relocation and dispersal occurred during the tests with higher burnup fuel. Similar fragmentation had been observed in LOCA tests with very high burnup rods performed in the Halden multi-lateral program. Several hypotheses regarding fuel fragmentation and dispersal were proposed, but none of them has been investigated yet.

The focus of SCIP III was on LOCA issues, in particular on fuel fragmentation, relocation and release. The influence of burnup, cladding strain, temperature, rod internal pressure and free volume and of micro-structural effects were assessed. The consequences of cladding overheating due to off-normal transients at lower than LOCA-typical temperatures and its impact on mechanical cladding properties was addressed as well. Finally, the impact of axial constraint on fuel rod performance during a LOCA transient was investigated.

In a second Task, PCMI and PCI issues were further studied, amongst others the potentially beneficial effect of slow and staircase ramps compared with fast ramps leading to PCI failure.

With one exception, modelling had not been part of SCIP and SCIP II. Instead, it had been performed by project participants on a voluntary basis and discussed during modelling workshops. Although providing a large amount of valuable results and insights, the approach also clearly demonstrated the limitations of such voluntary efforts and the obvious need to support an experimental program like SCIP III. Therefore, modelling was an integral part of SCIP III. In addition, support was provided by an internal and an external expert group.

Like the earlier projects, SCIP IV is planned to be a five-year program with an overall budget in the order of 14 M€ (SCIP III fee +10%), starting in July 2019. It will be organised in a similar way as SCIP III. The present report describes potential Tasks and Subtasks of SCIP IV as a basis for discussions within potential participants' organisations.

In total, 19 Subtasks are described in the present proposal. Eight Subtasks within Task 1 aim at studying fuel and cladding performance issues related to interim storage. The seven Subtasks described under Task 2 represent a continuation and extension of work performed in SCIP III to investigate LOCA issues. Even Task 3 is a continuation and extension of work performed in SCIP III related to PCI. As in SCIP III, modelling efforts supporting planning and interpretation of experiments in Tasks 1 – 3 will be concentrated in a dedicated Task. Performing all work would exceed by far the SCIP IV budget. Therefore, the interaction with potential participants is expected to provide a prioritisation that will allow defining the final scope of work within the disposable resources.

Based on the results of the prioritisation exercise, the present report will be revised and transformed into a technical description of SCIP IV, which will form the basis for potential participants to take the decision for joining the new project.

The potential topics of the technical program of SCIP IV, as it is described in detail in this document, are summarised below:

Task 1 Back end

Subtask 1.1 – Cladding creep and creep failure limits in dry storage:

Under interim dry storage conditions, the cladding is under tensile hoop stress. Since it is expected that spent fuel will be stored for long periods of time, long term creep is a relevant deformation mechanism when assessing fuel rod integrity. When fuel assemblies are loaded into dry storage casks, repeated vacuum drying is applied, which leads to cyclic load. Within this subtask, the temperature and hoop stress dependence of the secondary creep rate will be investigated for different materials (defueled irradiated cladding samples from rods with different burnups).

Moreover, the process of vacuum drying that leads to temperature and pressure cycling will be assessed.

Subtask 1.2 – In-storage annealing: creep acceleration and ductility change:

Fuel cladding temperatures under dry storage conditions might be high enough for irradiation damage to be annealed. This might favour creep acceleration. Conditions that could lead to accelerated creep during dry storage and the ductility change that accompanies it will be studied.

Subtask 1.3 – Creep of fuel rods under simulated dry storage conditions:

Whereas many creep and hydride reorientation tests of unirradiated cladding have been performed, hardly any data are available on the thermal creep properties of irradiated fuel rods with fuel pellets inside. In high burnup fuel rods, fuel-cladding bonding could restrict cladding creep out. In addition to the effects on creep behaviour, bonding might also affect hydride reorientation behaviour in the cladding, leading to local stress concentrations favouring local hydride reorientation and creating potential spots vulnerable to crack initiation and propagation under long-term dry storage conditions. Possible effects due to fuel-cladding bonding in high burnup fuel rods will be investigated. Creep properties of rod segments with fuel inside will be compared to defueled cladding properties. Potential hydride reorientation will be assessed and mechanical properties of the cladding before and after creep testing will be determined.

Subtask 1.4 – Special fuel rods:

It is obvious that leaking fuel rods require non-standard handling procedures when transferred to interim dry storage. But in addition, there are non-leaking spent fuel rods around that might not be able to fulfil the required safety, regulatory or operating functions during post-operation, such as handling and storage. Thus, fuel with characteristics such as high cladding corrosion, thick crud layers, high hydrogen content, hydride blisters, high internal pressure, which may lead to radial hydrides, etc., may also be considered as weak and potentially ‘damaged’. As handling of ‘damaged’ fuel is much more complicated and expensive, compared to established standard procedures, classification of potentially vulnerable fuel rods is a key issue. Non-destructive inspection techniques supporting this classification will be evaluated and tested. Mechanical properties of weakened and damaged fuel rods will be determined, to establish criteria, which ensure integrity during back-end handling, transport and intermediate storage.

Subtask 1.5 – Hydride reorientation:

During back end handling and dry storage, fuel cladding temperatures will be high enough to dissolve hydride precipitates back into solid solution. When temperature drops later on, hydrogen will be precipitated again. If the cladding is under high enough hoop stress, the precipitated hydrides will be oriented in radial direction, which impacts ductile-to-

brittle transition behaviour of the cladding material of concern. The conditions and mechanism for hydride reorientation in irradiated cladding material will be determined, in order to predict both the hydride reorientation and ductile-to-brittle transition behaviour of the material, based on the understanding of these parameters.

Subtask 1.6 – Delayed hydride failure during interim storage:

It is well known that sensitivity to hydride induced failures in Zirconium alloys increases at lower temperatures. Two types of hydride induced failure mechanisms have been observed in zirconium alloys; classical hydrogen embrittlement that acts on the macroscopic scale, and delayed hydride cracking that acts locally, in front of a stress concentrator. Delayed hydrogen cracking is a time-dependent mechanism that acts on a local level in front of stress concentrators. It operates at much lower macroscopic hydrogen and stress levels than classical hydride embrittlement and is therefore relevant for all fuel rods. It occurs, if the hydrogen concentration is high enough, if temperature is below a material specific maximum value, if there is sufficient time for a crack to propagate through the cladding wall, and finally, if stress intensity is above a critical value. For most rods, the three first conditions are fulfilled under back end conditions. Thus, it depends on the value of the critical stress intensity factor whether or not delayed hydride cracking occurs. The subtask aims at determining critical stress intensity factors for irradiated fuel cladding in the temperature range 150-400 °C. Based on the results, the critical (maximum) length of flaws in the cladding will be determined at internal pressures typical for back end conditions. The effect of impact/bending on delayed hydride cracking will be investigated, by performing bending or impact tests on fuel rods with blisters and/or radial hydrides followed by a constant load.

Subtask 1.7 – Spent fuel rods in transport and handling operations and in accident scenarios:

Independent from the back end concept, fuel assemblies are handled, loaded into transport casks and unloaded or stored in dry-storage casks when removed from the on-site spent fuel pool. A very large number of transports have been performed successfully worldwide. Only for special transportation conditions or accident situations is there a substantial need to verify spent fuel behaviour and suitability for further storage. This subtask will concentrate on four areas of concern. It aims at generating valuable experimental data on the mechanical response of irradiated fuel rods under transport accident conditions. The data will support analytical models for regulatory accident evaluation. In addition, they will also be useful for seismic and vibratory evaluations. In order to support cask containment analysis and the definition of source terms for accident scenarios, the particulates which might be released from high burnup fuel rods due to impact events will be characterised. The third objective is to investigate the potential effects of handling and transportation of low burnup fuel and verify its safe reuse after transportation. Finally, the

strength of weak or slightly damaged fuel rods under transportation and handling operations will be investigated. The aim is to verify that weak or slightly damaged rods will not degrade or jeopardise cask safety functions during transportation and storage.

Subtask 1.8 – Failed fuel:

In most countries, no standard procedures have yet been established to take care of failed fuel for interim storage and final disposal. For safe long-term stabilisation of failed fuel, the radiological confinement needs to be restored and the geometry and environment needs to be controlled and stable. There are different concepts available to encapsulate damaged and failed fuel rods, either by canning in-pool or by conditioning and encapsulation at a hot cell. In this context, drying of failed fuel is essential to avoid gas generation by radiolysis of residual water and moisture. The presence of oxygen and hydrogen gas could have undesirable consequences, such as oxidation of the fuel, hydriding of the cladding, corrosion and pressure build-up. Whereas standards have been established for drying of intact spent fuel in dry storage casks, for failed fuel these standard drying procedures may not be sufficient to guarantee the required moisture level for encapsulation. Therefore, test methods to measure moisture content need to be developed and validated to prove that criteria on moisture content can be met. Furthermore, available drying procedures need to be evaluated for failed fuel and possibly optimised. Within this subtask, experimental data on the issue of safe encapsulation and storage of failed fuel rods will be generated, using established characterisation methods and assessment of residual water.

Task 2 Loss-of-coolant accidents

Subtask 2.1 – Microstructure related to fuel fragmentation:

The existence of a burnup threshold for fuel fragmentation in LOCA scenarios has been a key question in several studies and research efforts. As the experimental evidence grows, it seems that high burnup is only one of several factors determining the susceptibility of the fuel to fragment. Several hypotheses have been brought forward to explain this behaviour, such as effects of the power history inducing residual stresses in the pellet, or repartitioning of the fission gas inventory to closed grain boundary networks or bubble populations that weakens the integrity of the fuel under a LOCA event. Recent results from SCIP III have identified *some potentially very important effects (SCIP III proprietary information deleted)*. In order to study this potentially important phenomenon further, it is proposed to continue on the advanced microscopy examinations performed in SCIP III on fuels with high burnup that fragment to a large extent in LOCA like conditions, as well as to study high burnup fuel that appears resistant to fine fragmentation.

Subtask 2.2 – Fuel fragmentation, relocation and dispersal in non-standard fuel:

In SCIP III, investigations focused on the performance of “standard

fuel”, i.e. UO₂ fuel with relatively small grains, whereas use of large grain fuel with dopants or additives has become more and more common. Moreover, the microstructure of MOX and gadolinia fuel might also develop differently during reactor operation, compared to standard fuel. Work to be performed under this subtask aims at extending data base and understanding of fuel fragmentation, relocation and dispersal to fuel types that have not yet been investigated within SCIP III or elsewhere. The data will support estimates of fuel dispersal in LOCA safety assessments carried out by utilities and regulators, as well as refinement and extension of fuel fragmentation models to be incorporated in fuel performance and transient codes.

Subtask 2.3 – Separate effects tests:

Tests in SCIP III have indicated that for fuels susceptible to fine fragmentation critical parameters may be both the temperature ramp rate and the magnitude of the depressurisation transient upon burst. The possibility to control temperature ramp rates was rather limited in SCIP III heating tests. Therefore, it is proposed that a new furnace is constructed to better control the temperature ramp rate in tests of similar size as the existing heating test apparatus (testing a few pellets worth of material). The equipment will be made compatible with a new depressurisation rig being able to simulate the burst event with high degree of control, including an expansion chamber to contain and collect the ejected fuel fragments for further study. Once critical parameters have been identified, a few integral LOCA tests might be performed to verify the results.

Subtask 2.4 – Fuel and cladding oxidation in LOCA:

Results from LOCA tests performed in SCIP III that focused on the impact of high temperature steam oxidation on mechanical properties of the cladding indicated that corrosion performance might be influenced by the pre-test oxide layer. Starting from these data, more detailed studies will be performed, consisting of high temperature oxidation tests with fuel rod samples with and without fuel, followed by corresponding post-test characterisation, in order to compare performance of irradiated cladding with unirradiated material tested under the same conditions. In addition, potential oxygen uptake from the irradiated fuel can be assessed. During a small break LOCA, oxidation of Zircaloy can occur at high pressure, whereas most steam oxidation tests reported in the literature have been carried out at atmospheric pressure. Tests with unirradiated material in a temperature range of 750-1000 °C indicated an effect of steam pressure on oxidation kinetics. High temperature oxidation on irradiated cladding at different steam pressures will be studied within this subtask by means of new test equipment. The results will support establishing a correlation to calculate ECR values at steam conditions relevant for small break LOCAs. After burst in a small break LOCA, the fuel will be exposed to steam and/or water, which might lead to oxidation of uranium, increasing its solubility and the release of radionuclides to the system. Fragmented fuel will be characterised by means of XRD, in order to identify oxidised

uranium oxide phases such as U_3O_8 . Oxygen profiles in fuel pellets that did not exhibit severe fragmentation will be determined. Oxidation tests with dedicated equipment to be developed might also be performed on single pellets with cladding.

Subtask 2.5 – Spent fuel pool LOCA:

Loss of coolant in a spent fuel pool, with high temperature oxidation of cladding in an air-steam mixture as well as transients leading to ballooning and burst of fuel rods, can have severe consequences. Within SCIP III, only two LOCA tests under simulated spent fuel pool conditions have been performed. Moreover, the scope of post-test examinations was rather limited. Therefore, additional spent fuel pool LOCA tests, covering a broader band of potential conditions, will be performed in this subtask. The scope of post-test examinations will be extended, providing additional data to define the fission product source term for this type of events.

Subtask 2.6 – Post LOCA seismic loads:

Post-LOCA seismic loads have been identified as a potential accident scenario that could challenge core coolability and safety of a nuclear power plant. In SCIP III, a device for integral LOCA tests has been developed that is able to study fuel rod resistance to axial loads after ballooning, burst and high temperature oxidations. This equipment can be used to produce specimens for seismic load experiments. Fuel rod segments will be subjected to LOCA transients including balloon, burst, high temperature oxidation and quench. Afterwards, the segments will be tested by 4-point bend tests or by axial load tests to simulate post-transient seismic loads. Material and transient conditions will be chosen in a way that allows determining fuel rod seismic failure limits and comparing results with literature data on non-irradiated material. The data will support estimates of fuel rod resistance to seismic loads in LOCA safety assessments. The results might also be useful for fuel handling guidelines after a LOCA. Moreover, they will indicate, how representative data on non-irradiated and on defueled material are, compared to rods with fuel.

Subtask 2.7 – Transient fission gas release and axial gas communication:

During a loss-of-coolant accident, rapid and large changes of temperature may cause transient fission gas release from the fuel, by mechanisms such as fuel grain boundary fracture or diffusion and interconnection of fission gas bubbles. Understanding of the transient fission gas behaviour is important to determine factors such as increase in rod inner pressure and margins to cladding burst and loss of rod integrity. Knowledge of the transient fission gas release also allows for a more accurate determination of the source term in an accident scenario. In order to properly assess the effects of transient fission gas release on local pressure and ballooning and burst, it is important to know the axial gas communication inside the fuel rod. As a continuation of a limited number of tests performed in SCIP III, it is proposed to perform a parametric study of axial gas communication against burnup and temperature. The results will support im-

proving fuel performance code models of gas communication under transient conditions.

Task 3 – Pellet-cladding interaction

Subtask 3.1 – Data for modelling:

Fuel performance codes use different methods and criteria to determine when a PCI failure occurs. One of them is based on the cumulative damage index, defined by means of out-of-pile stress corrosion cracking data. Data for standard Zircaloy-2 and Zircaloy-4 cladding have been available for many years, but little or no data on more modern cladding materials are available. This subtask aims at obtaining stress corrosion cracking time-to-failure data for irradiated cladding tubes of modern materials. The data will also be evaluated, compared to existing data and put into a form suitable for use in fuel performance codes. Model calculations can then be performed and the damage predictions with the new dataset can be compared to those based on the old set and also applied to SCIP ramp tests.

Subtask 3.2 – Chemistry:

It is a given fact that iodine is an active agent in stress corrosion cracking, leading to PCI fuel rod failures. An issue that is far from having been elucidated is the timing of release of active fission products relative to the mechanical load of the cladding. From ramp tests, it is difficult, if not impossible to gain insight into this issue; therefore, it has to be investigated by means of laboratory experiments like mandrel tests with equipment that allows controlling the iodine level and its variation with time. In addition to a series of mandrel tests that investigate the influence of the timing of iodine ingress, it is proposed that the SCIP III database on the mitigating effect of oxygen is further extended.

Subtask 3.3 – Microstructure and microchemistry:

The importance of chemically active agents for stress corrosion cracking is well recognised, but mode of action of these species, their way to and their distribution at the location of concern, their chemical and physical form and many other aspects are still not well understood. SCIP III collaboration with the University of Manchester led to promising results. Within this subtask, microstructure and microchemistry inside cracks and at the crack tip of irradiated cladding samples that had experienced stress corrosion cracking will be investigated by means of advanced techniques in collaboration with external partners.

Subtask 3.4 – Operational parameters:

The parameter study on the timing of iodine ingress in Subtask 3.2 will hopefully reveal some correlations between transient parameters, availability of active agent and susceptibility to SCC. This subtask will verify these findings by means of 2-4 ramp tests performed in the Halden ramp test rig. The inventory of active agents will be controlled by an extended period of conditioning (several months) at low power. Planning of the tests will be supported by modelling.

Task 4 – Modelling

This task aims at supporting SCIP IV with pre- and post-test modelling calculations of tests and experiments using different codes and models. More specifically, the objectives are to provide input to the design of test matrices and to the selection of test parameters, to improve the evaluation and interpretation of experimental results, to extend the basis for the validation of existing models and to identify model improvements and the data needs for such improvements.

1 Introduction

The fuel rod cladding fulfils an important barrier function, amongst others during normal reactor operation and anticipated operational occurrences (AOOs) as well as during backend handling including transport and dry storage. It prevents fission products and actinides from being released into the reactor coolant or into transport and storage equipment. Under design basis accident conditions like loss-of-coolant (LOCA) and reactivity initiated accidents (RIA), both fuel and cladding integrity are important for ensuring safe shutdown and for maintaining subcriticality and a coolable geometry of the reactor core.

Although fuel rod failure rates have decreased considerably over the years, the significance of a single failure and of its consequential costs is much higher in today's competitive environment. On the other hand, unnecessary operational limitations, maintained in order to reduce the risk for potential fuel rod failures, should be eliminated in order to reduce fuel cycle costs. This is only possible, if failure mechanisms are understood and can be modelled quantitatively.

The Studsvik Cladding Integrity Project, SCIP, was launched in 2004. It was a five year OECD/NEA Joint Project operated by Studsvik with about 30 participating organisations, including regulatory bodies, research institutions, utilities and fuel suppliers from 13 different countries. SCIP aimed at studying basic phenomena of fuel rod failures driven by pellet-cladding mechanical interaction, thus contributing to a better understanding of fundamental failure mechanisms. Pellet-cladding mechanical interaction, primarily as a function of burnup, was studied in a number of ramp tests. Key parameters important for hydrogen induced failures, in particular delayed hydride cracking and failures due to embrittlement of the cladding as a consequence of hydriding, are now much better understood thanks to SCIP and could in many cases be quantified. In the case of failures caused by stress corrosion cracking from the inside of the fuel rod ("classical" pellet-cladding interaction, PCI), equipment simulating in-core conditions was significantly improved.

From the very beginning, SCIP prioritised studies on cladding. Studies on pellet-related parameters were in general not considered. Early in SCIP it became obvious that pellet properties, dramatically changing with burnup, need to be considered as well in an integral description of PCI/PCMI. Furthermore, all fuel vendors were also in the process of developing advanced fuel types with additives or dopants and large grains. One of the expected advantages of these new fuel types was to reduce and mitigate the risk for PCI in AOOs. Consequently, the 5-year continuation of SCIP, SCIP II, aimed at improving the knowledge on the role of the fuel pellet related to fuel failures driven by pellet-cladding mechanical interaction (PCMI).

The four Tasks of SCIP II dealt with a review of old ramp test results, with pellet-cladding mechanical interaction, with chemically assisted stress corrosion cracking (pellet-cladding interaction, PCI) and, as a carry-over and continuation of work performed in SCIP I, with hydrogen-induced failures. The pellet behaviour was assessed in power ramp tests. Performance of advanced fuel types with additives or dopants and large grains, compared with standard fuel, was assessed by means of the most advanced available examination techniques. This included the application of Laser-Ablation in combination with Inductively Coupled Plasma Mass Spectrometry (LA-ICP-MS), modern Scanning Electron Microscopy (SEM) with Electron Back Scattered Diffraction (EBSD) and Transmission Electron Microscopy (TEM). SCIP II delivered a huge amount of data and knowledge on the behaviour of advanced fuel under power transient conditions.

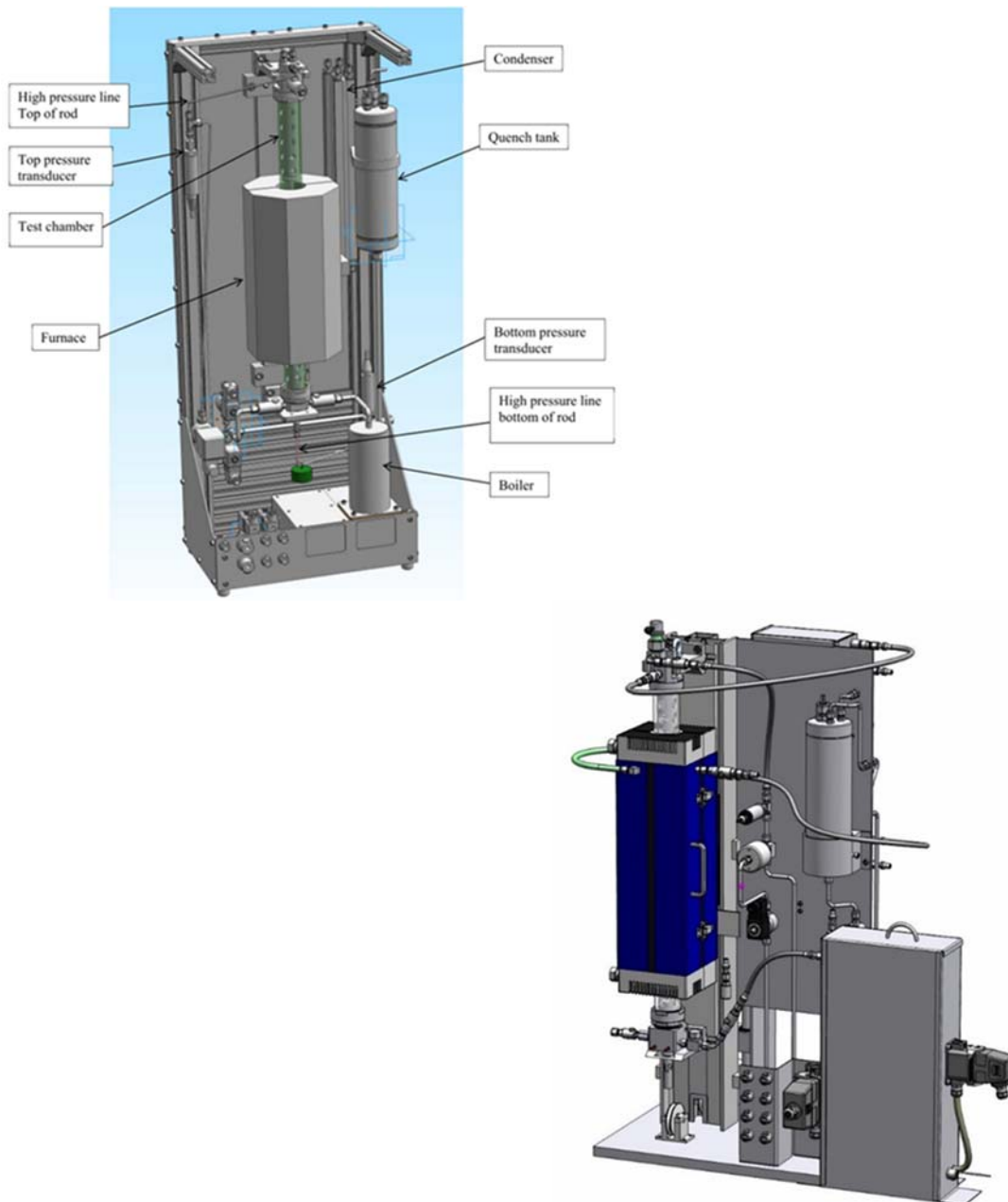
Simultaneously with SCIP II, the U.S.NRC charged Studsvik with a LOCA test program and chose the SCIP II Program Review Group as an advisory board. In this program, six single-rod integral LOCA tests were performed, basically following the same procedures as applied by the Argonne National Laboratory in earlier campaigns. Significant fuel fragmentation, relocation and dispersal occurred in tests with higher burnup, whereas no fuel was expelled during the tests at lower burnup. Similar fragmentation behaviour had been observed in LOCA tests performed in the Halden multilateral program with very high burnup rods.

The observation of fine fragmentation in these tests demonstrated the need to investigate this phenomenon in more detail. One of the conclusions of a comprehensive review of LOCA research programs by the U.S.NRC, covering the results of more than 90 LOCA tests, was that “more research and detailed analyses are required to determine the extent of fuel loss, evaluate the identified consequences, and ensure that the identified consequences are comprehensive, complete, and within the regulatory envelope.” In response to this need, SCIP III, the next five-year program extension ending in 2019, focuses on issues related to fuel fragmentation, relocation and dispersal (FFRD). The degree of fragmentation and the size distribution of the fragments are important parameters determining the amount of fuel that might be released through a rupture in the ballooned zone of a fuel rod exposed to a LOCA. Furthermore, the understanding of mechanisms behind fuel fragmentation and dispersal in LOCA transients is supported. Two test methods are used to investigate these issues, furnace heating tests and integral LOCA tests.

Heating tests revealed ... (*SCIP III proprietary information deleted*).

Regarding last cycle power and burnup threshold, no obvious correlation between end-of-life power, burnup and fragmentation has been identified so far.

Integral LOCA tests are performed in two test devices installed in the Studsvik hot cell (Figure 1).

**Figure 1**

Old (left) and new (right) integral LOCA test device

Heating test results show the importance of cladding restraint on fuel fragmentation. LOCA post-test gamma scans provide information on fuel fragmentation, relocation and dispersal, whereas profilometry gives the strain profile. Combining these two allows determining the cladding strain, where FFRD can be observed (Figure 2). An average strain threshold value of ... (*SCIP III proprietary information deleted*).

Fuel dispersal depends on the degree of fragmentation and on the size of the burst opening. Almost ... (*SCIP III proprietary information deleted*).

The comparison of burst and non-burst LOCA tests performed with samples from the same fuel rod shows the importance of the depressurisation shock as an initiator of fuel fragmentation. Some more integral LOCA tests with varying fill gas pressure and plenum volume are planned soon.

... (*Figure containing SCIP III proprietary information deleted*).

Figure 2

Comparison of gamma scan and profilometry results from a LOCA tested rodlet

There is a range of events in nuclear reactors which result in a mismatch between power and the available cooling. Insufficient cooling leads to loss of the coolant film and to cladding overheating for a short time (less than a few seconds) or a longer duration, up to a few hundred seconds, before the cladding is rewetted. Depending on the peak cladding temperature and the duration of the overheating, the consequences for the fuel range from negligible to severe loss of fuel integrity. Examples of such anticipated operational occurrences (AOOs) are loss of power to all recirculation pumps, tripping of the turbine generator set, isolation of the main condenser, and loss of all offsite power. They are expected to occur once or several times during the lifetime of a nuclear power plant. Consequences of such off-normal temperature transients are studied within SCIP III as well, investigating transients, where the tightness of the cladding is maintained, but with a potential impact on material properties that might require non-standard procedures for handling, transport and storage. Such non-standard procedures can have severe economic consequences. The work aims at defining criteria for classifying fuel rods as undamaged or damaged, where damaged fuel would require non-standard handling, transport and storage procedures. A study of loss-of-coolant transients in a spent-fuel-pool by overheating in an air-steam mixture is also part of SCIP III. None of the tests is yet fully evaluated.

During a loss-of-coolant accident, the rapid and large changes of temperature cause the fuel rod to first expand axially, when the temperature increases, and later to contract upon cooling and quenching. If the contraction of the rods is hindered, tensile load would be imposed on the fuel rods. A rapid temperature drop and axial contraction are especially likely to occur during quenching. Thus, a fuel rod with a restricted axial contraction under quenching undergoes a thermal shock, because it simultaneously meets axial loading and a rapid drop of temperature. Restrictions on the axial contraction of fuel rods by rod-to-grid linkage could be caused by cladding ballooning in vicinity of spacer grids, by high temperature formation of a eutectic between the zirconium alloys and the Inconel rod springs; which may bond the cladding to the grid upon cooling, or by friction between fuel rods and spacer grid. In addition, in PWR assemblies, the spacer grids are fixed to the guide tubes. It is also possible for the fuel rods to interact with each other by bending or ballooning, which also may lead to axial loads. In response to this issue a study of

fuel performance in a LOCA transient under axial load is included in the SCIP III program. The objective of this work is to determine the threshold for fuel break in terms of oxidation (ECR) and axial load for fuel of different burnups. Test results are under evaluation.

The main fuel failure mechanism studied in SCIP II was PCI in power ramps. SCIP II generated a large amount of new data and knowledge on PCI and in particular on the chemistry effects and the behaviour of advanced fuel types. Nevertheless, there were still a number of open issues to be investigated. Therefore, PCI issues are further studied in SCIP III. The main study is related to the beneficial effect of slow ramp rates. This is investigated using mandrel testing, complemented by some in-pile ramp tests. Detailed post-ramp examinations concentrate on the pellet-cladding interface, including bonding and inner oxide layers as well as cracks in the fuel pellet and incipient cracks in the cladding inner surface.

With one exception, modelling has not been part of SCIP and SCIP II. Instead, it was performed by project participants on a voluntary basis and discussed during modelling workshops. Although providing a large amount of valuable results and insights, the approach also clearly demonstrated the limitations of such voluntary efforts and the obvious need to support an experimental program like SCIP III by modelling as an integral part of the work. Therefore, modelling is now an integrated part of SCIP III. Several external parties are bilaterally supporting this effort. In addition, all participants are invited and encouraged to participate on a voluntary basis to get a broad and rewarding discussion in place. Results from modelling exercises are presented and discussed in modelling workshops. SCIP III is not supposed to develop any codes or parts of codes by itself, but to facilitate code development by generating high quality experimental data, which can be used in support of the participants' code development. In addition, modelling supports experimental work planning in SCIP III. Amongst others, the following codes have been used for modelling work related to SCIP III:

ALCYONE, COPERNIC, DRACCAR, ENIGMA, FRAPCON, FRAPCON-QT, JASMINE, RELAP and TRANSURANUS

One objective of modelling is to compare results from base irradiation modelling with results from post-irradiation examinations. Another objective was to compare results from LOCA modelling with test results. Both were done at a Modelling Workshop at the SCIP meeting in November 2017.

In general, code results agreed quite well with examination data. There were some differences for porosity and gas distribution. Code predictions of Studsvik LOCA test results for failure/no failure, burst pressure, burst temperature and peak strain agreed quite well, but most codes are missing models for important parameters for predicting fuel fragmentation, relocation and dispersal.

A complementary modelling workshop session is planned at one of the next SCIP meetings, focusing on PCI issues and ramp tests.

Like the earlier projects, SCIP IV is planned to be a five-year program with an overall budget in the order of 14 M€ (SCIP III fee +10 %), starting in July 2019. It will be organised in a similar way as SCIP III. The present report describes potential Tasks and Subtasks of SCIP IV as a basis for discussions within potential participants' organisations.

In total, 19 Subtasks are described in the present proposal. Eight Subtasks within Task 1 aim at studying fuel and cladding performance issues related to interim storage. The seven Subtasks described under Task 2 represent a continuation and extension of work performed in SCIP III to investigate LOCA issues. Even Task 3 is a continuation and extension of work performed in SCIP III related to PCI. As in SCIP III, modelling efforts supporting planning and interpretation of experiments in Tasks 1 – 3 will be concentrated in a dedicated Task. Performing all described tasks would exceed by far the SCIP IV budget. Therefore, the interaction with potential participants is supposed to provide a prioritisation that will allow defining the final scope of work within the disposable resources.

Based on the results of the prioritisation exercise, the present report will be revised and transformed into a technical description of SCIP IV, which will form the basis for potential participants to take the decision for joining the new project.

One of the important roles of SCIP has been establishing an international forum for the interaction between fuel suppliers, utilities, research institutions and authorities. This has been a very successful part of the SCIP program and it continues to play the same role in SCIP IV. The interaction is illustrated in Figure 3.

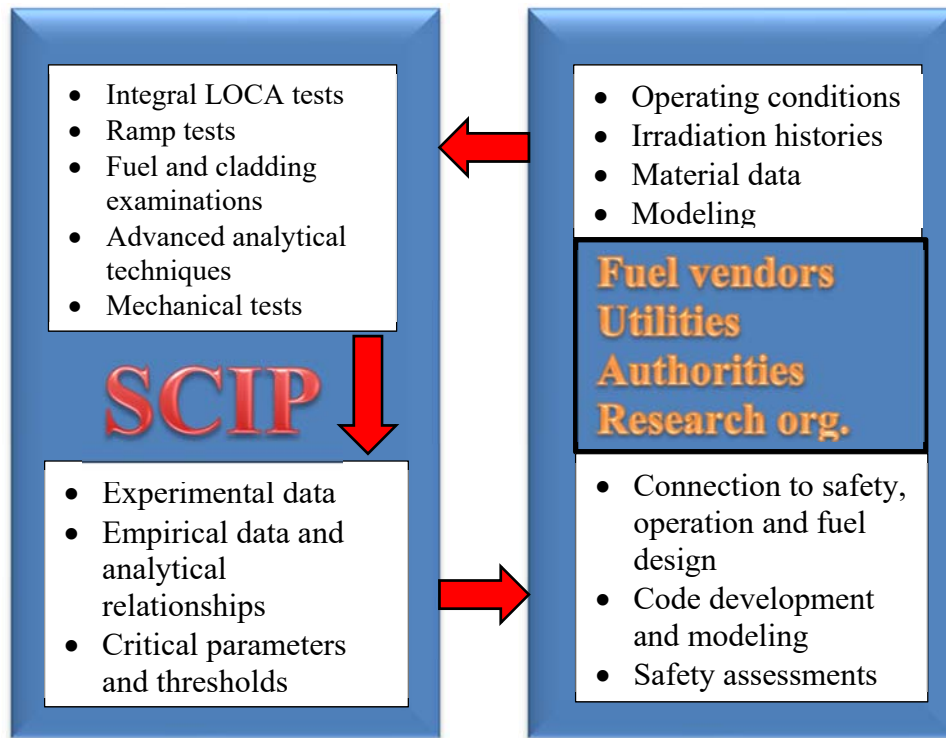


Figure 3
The role of SCIP interacting with industry partners and authorities

2 Technical description

2.1 Task 1 Back end

2.1.1 Subtask 1.1 – Cladding creep and creep failure limits in dry storage

Main author: Cecilia Janzon

Background

Long term interim storage is a consequence of the fact that final disposal of spent nuclear fuel (SNF) is not yet available in a number of countries [1]. Since it is expected that spent fuel will be stored for long periods of time, long term creep is a relevant deformation mechanism when assessing fuel rod integrity.

Creep deformation [2] is a slow time dependent deformation that occurs when materials are subjected to stresses lower than the yield stress for an extended period of time. The material adjusts itself to the applied force by displacing atoms and atomic planes, in order to reduce stress. When the displacements are large enough, a continuous deformation can be observed macroscopically, the so called strain. The strain depends on the stress state, the temperature and on previously accumulated strain.

Creep is commonly represented by the creep – rupture curve that depicts strain as a function of time until rupture. Creep exhibits three stages (Figure 4):

- Primary creep with decreasing strain rate
- Secondary (or steady state) creep with approximately constant creep rate
- Tertiary creep with increasing strain rate

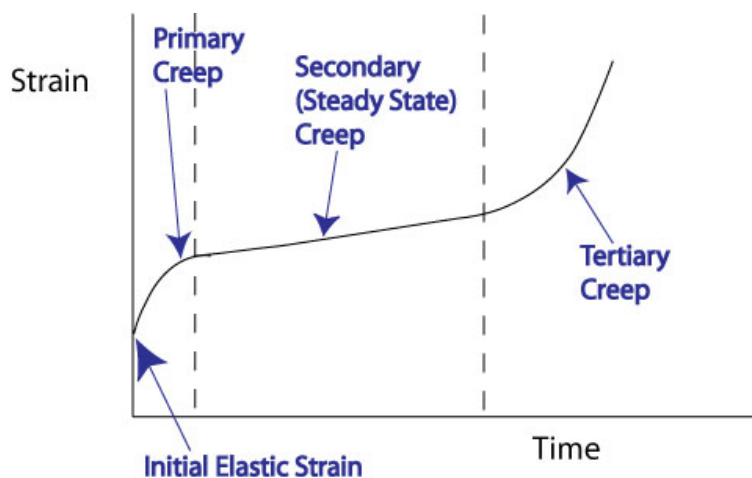


Figure 4

Schematic representation of strain/time behaviour under creep conditions

After irradiation, the fuel rod cladding will experience tensile hoop stress due to larger rod internal pressure than ambient. The pressure will also be larger than the as-fabricated fill pressure due to release of fission gas and decrease of the free volume.

When fuel assemblies are loaded into dry storage casks, vacuum drying is applied, which temporarily deteriorates heat transfer. Thus, the cladding temperature may reach temperatures close to 500 °C. This in turn increases the tensile hoop stress due to the increasing rod internal pressure. Thus, significant creep strain may be induced by the vacuum drying alone. Once the dry storage cask is back-filled with inert gas, the fuel temperature drops again and will thereafter slowly decrease due to the diminishing decay heat. During dry storage, typical conditions are temperatures up to about 400 °C and hoop stresses around 120 MPa. Dry storage regulations vary slightly between different countries; the lowest limits for dry storage are 370 °C (Germany) and 90 MPa for cladding hoop stress (USA and Spain). In a few countries, cladding strain is limited to 1 % [3].

Over the years Studsvik and other hot cell laboratories have performed thermal creep tests and collected creep data on irradiated cladding. However, the number of test samples has typically been quite limited in each test campaign and there are data gaps to be filled. Furthermore, there are new cladding materials being introduced for which no or very limited irradiated creep data exists.

Objectives

Investigate the temperature and hoop stress dependence of the secondary creep rate for different irradiated cladding materials. Creep test samples will be fabricated from fuel rods with different burnups.

Investigate the effect of vacuum drying by temperature and pressure cycling as illustrated in Figure 5.

Experimental

Studsvik has long experience in performing creep testing of irradiated cladding samples.

Biaxial creep tests are performed on cladding tube specimens with welded end plugs (PROVFAB specimens). The specimen is placed in a furnace and internally pressurised by gas at constant pressure. The resulting diametrical deformation is measured as a function of time.

With corresponding temperature calibration, the tests can be performed at different temperatures.

The diameter is measured by a high resolution laser micrometre. Furnace and laser setup inside the cell is illustrated in the cutaway drawing in Figure 6. The furnace is shown with a specimen mounted at the measurement position and connected to the pressurisation line. Laser sender and receiver are shown on opposite sides of the furnace. The laser measures

the diameter of the sample at mid-height of the cladding between the rigid support rings.

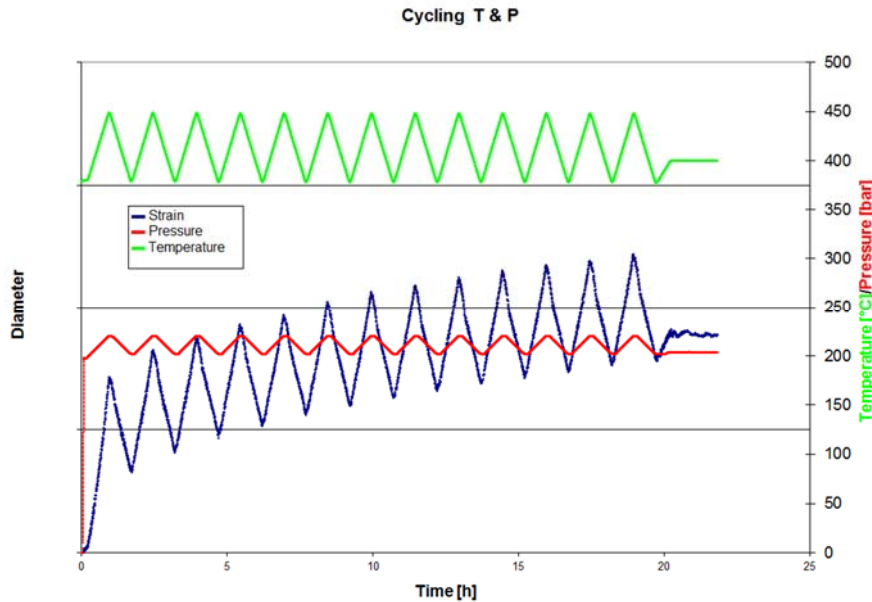


Figure 5
Simulation of thermal creep during vacuum drying

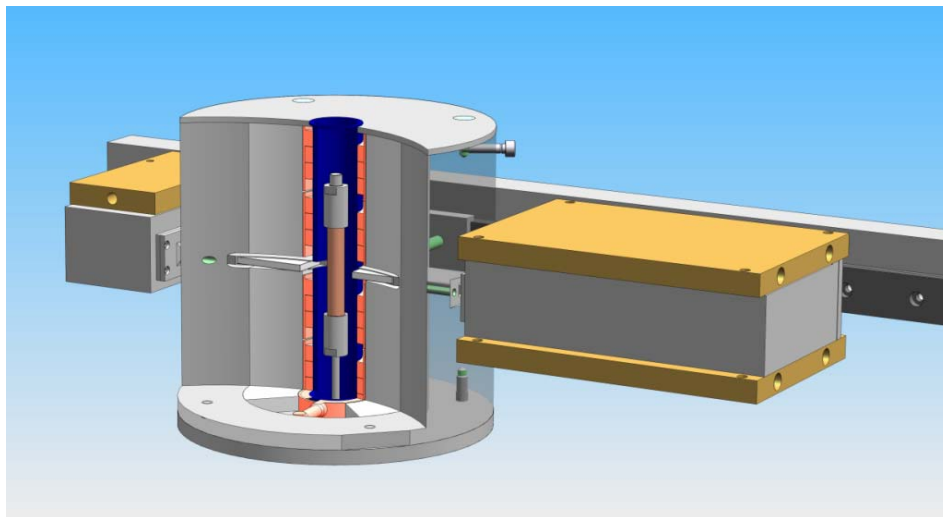


Figure 6
Schematic view of creep furnace and laser measurement equipment

Pre-test characterisation

The pre-test characterisation will include gamma scanning, profilometry and oxide thickness measurements. The hydrogen concentration will be determined and the hydride morphology will be characterised by microscopy.

Test matrix

A preliminary test matrix is presented in Table 1. Tests will typically be performed at three different temperatures and three different stress values, in total 5-7 creep tests per material condition.

One or two tests will be performed with simulated vacuum drying conditions prior to the creep test.

Some tests will be performed to simulate the temperature decrease under stress to allow hydride reorientation to occur. This will provide some samples for Subtask 1.5 on hydride reorientation (Section 2.1.5).

Table 1

Preliminary test matrix for creep testing

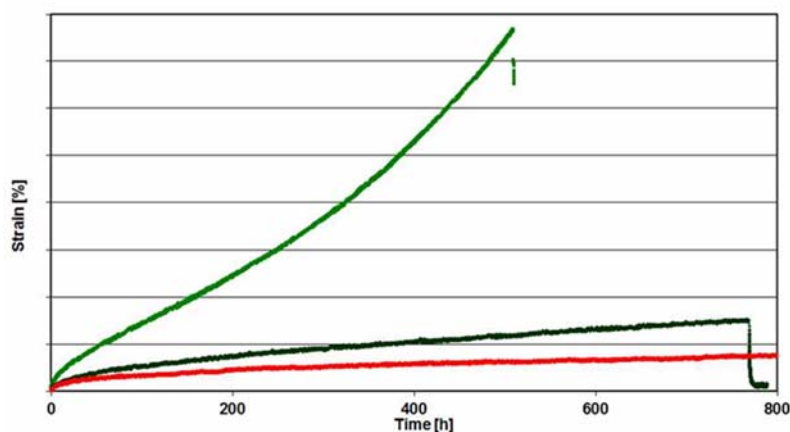
Material	Burnup [MWd/kgU]	Hydrogen conc. [ppm]	Temperature [°C]	Hoop stress [MPa]
PWR	30-55	100-400	350-420	120-180
BWR	30-55	100-400	350-420	120-180

Post-test characterization

Post-test characterisation will include profilometry and possibly microscopy for hydride morphology.

The deliverables will be:

- Creep test curve showing the diameter or strain of the specimen as a function of test time. An example is shown in Figure 7.
- Secondary creep rate, evaluated and given in strain increase per hour [%/h].
- Strain evaluation from pre- and post-test profilometry

**Figure 7**

Example of creep test curves, showing strain as a function of time

2.1.2 Subtask 1.2 – In-storage annealing: creep acceleration and ductility change

Main author: Kwadwo Kese

Background

At the end of its service in the reactor and its cooling in the pool, the fuel cladding is under internal pressure from fission gases. The cladding material, as-irradiated, is characterised by high strength and low ductility, compared to the unirradiated state. The relative change in strength and deformation properties is the result of a change in the material's microstructure during irradiation in the reactor. This change involves irradiation damage in the form of microstructural defects, dislocation structure modification and the appearance of hydrides and an oxide layer. The defect microstructure consists of high-density small dislocation loops [4], while the hydrides are found as plates [5] distributed in the zirconium alloy matrix. The oxide on the other hand forms as a layer on the outside surface of the cladding.

During transportation and/or at the beginning of dry storage, the internal pressure may increase due to a rise in temperature resulting from fuel decay heat. If the rise in temperature is substantial, then annealing of the material may occur. The increased internal pressure translates into increased tangential stress in the cladding which, at elevated temperatures, could lead to creep of the material with cladding failure as a possible consequence. In this context, cladding failure may consist in cladding rupture or the expansion of the cladding diameter that precedes rupture. Rupture ends the creep process in the tertiary stage when a breach occurs in the material. Even if rupture does not occur, but the temperature starts to decrease while the cladding is under tangential stress, re-precipitation of hydrides with a radial orientation on the transverse cross-section will occur [6][7].

The U.S.NRC has set a temperature limit for normal storage and fuel loading operations at 400 °C and a tangential stress of 90 MPa for all fuel burnup levels. The temperature and stress limits, apart from ensuring that excessive creep is prevented, are also intended to minimise the extent of hydride reorientation that might otherwise occur. For irradiated materials, recovery of irradiation hardening (or material 'softening') can occur if creep takes place at high enough temperatures, where annealing of irradiation damage may occur. Such a situation has been observed to lead to relatively early imposition creep acceleration (involving an increasing rate of creep). Since creep in dry storage is a slow process, laboratory creep testing is typically accelerated to obtain relevant data for modelling in a reasonable time. The creep tests are typically accelerated by performing them at higher stress levels than those present in the dry storage casks. This means that existing creep data and models does not necessarily consider the long-term annealing properties of the material. Under severe conditions of temperature and/or pressure for example,

creep acceleration has been reported at strains as small as 0.005-0.01 [8]. The annealed condition favours ductile rupture when fracture occurs, and is preceded by a characteristic ballooning instability.

Objectives

The objective of this subtask is to study the conditions that could lead to creep acceleration during dry storage and the ductility change that accompanies it.

Experimental

Determination of threshold conditions for accelerated creep of irradiated cladding materials

By first performing an annealing step without rod internal pressure, the level of annealing can be controlled and matched to the levels of annealing expected to occur under dry storage. The creep test will then be performed by applying internal pressure to the tube specimen. With this method, the impact of annealing on the creep rate can be determined directly. The tests will be performed on a set of irradiated cladding materials with appropriate material type, burnup level and hydrogen content. If the same materials are chosen as in the Subtask 1.1 creep tests, then this subtask will generate reference data without the annealing step.

Sample fabrication techniques as well as equipment for generating creep data by applying internal pressure to cladding tube samples are already well established at Studsvik. For a description of the creep test technique employed in Studsvik, see Section 2.1.1.

For each material type, the threshold annealing conditions that lead to creep acceleration will be determined. This will shed light on the accelerated creep characteristics of the candidate material types.

Test Matrix

It is proposed to investigate one PWR material and one BWR material in the 40 – 60 GWd/tU burnup range in the context of this subtask. With the aim of being able to define the creep rate as a function of level of annealing, creep temperature and stress, a test matrix is presented in Table 2 for one such proposed material. Data for the highlighted matrix entries of the as-irradiated material are expected to be available from Subtask 1.1.

Table 2

Proposed test matrix for annealing and creep testing of one test material

Annealing %	Creep temperature [°C] (at constant stress = 150 MPa)		
	400	350	300
0 (as-irradiated)	X	X	X
30%	X	X	
60%	X	X	X
	Stress (MPa) (at constant temperature = 400°C)		
	120	80	
0 (as-irradiated)	X		
30%	X	X	
60%	X	X	

Measurement of change of deformation characteristics as an effect of accelerated creep

The effect of accelerated creep on the cladding materials will be measured through mechanical testing either in the form of tensile testing or ring compression testing or both. Through these tests the change in the deformation characteristics of the material, especially the ductility, will be established and compared for the materials and temperature and pressure conditions involved.

2.1.3 Subtask 1.3 – Creep of fuel rods under simulated dry storage conditions

Main author: Joakim Karlsson

Background

Many creep and hydride reorientation tests of unirradiated cladding have been performed by different research organisations. Much fewer tests have been made on irradiated cladding materials and there is a need to fill in gaps and add data to the database for different cladding materials and conditions. Furthermore, the tests on irradiated cladding have almost always been performed on defueled cladding tube samples. To our knowledge there is hardly any data available on the thermal creep properties of irradiated fuel rods with fuel pellets inside.

Biaxial creep tests are typically performed by internal gas pressurization of the cladding tube and observation of the resulting diametrical creep. Hoop stress in the cladding is applied unrestrained to the full cladding inner surface. However, in the case of high burnup fuel, the fuel is typically bonded to the cladding wall. For this case, measurements on defueled and empty cladding are most probably not representative of the real situation. It is expected that fuel-cladding bonding restricts cladding creep out. Thus, existing creep data from defueled samples might be on the conservative side. For modelling it is of interest to confirm the expected phenomenon of fuel-cladding restraint. The restraint may just decrease the initial creep rate, but it may also manifest itself as an incuba-

tion time before bonding breaks and lift-off occurs. The behaviour of fuel rods under internal pressure needs to be better understood. Measured data are also required for improvement of creep models for more accurate predictions of fuel rod creep in storage systems.

Apart from the inferred effects on creep behaviour, fuel-cladding bonding may also affect hydride reorientation behaviour in the cladding. In the absence of the fuel cladding gap, the internal gas pressure permeates through fuel cracks and exposes the cladding to local stress concentrations. Such local stress concentrations may be sufficient for local hydride reorientation and therefore, such locations may be vulnerable to crack initiation and propagation under long-term dry storage conditions. There are practically no measured data available on this potentially important aspect of fuel-cladding bonding and localised cladding stress.

Objectives

Investigate the possible effects due to fuel-cladding bonding in high burnup fuel rods. Such effects may include the existence of an incubation time, cladding lift-off and an altered creep rate.

Measure the creep properties with and without fuel-cladding bonding and with and without fuel pellets inside the cladding. Examine if localised hydride reorientation can occur and characterise the mechanical properties of the cladding before and after creep testing.

Experimental

Studsvik has long experience of performing creep testing of irradiated cladding samples. Only defueled specimens are accepted in the lead shielded cells, which house the current creep testing equipment. Tests on fuel rods without defueling require a new creep test system to be installed in the Studsvik hot cells.

A new creep test system with diameter measurement will be designed and installed in a hot cell. Such a system is sketched in Figure 8. The creep test specimens will be refabricated from suitable fuel rods with different cladding materials, burnups and hydrogen content. To prepare a specimen, a section will be cut from a fuel rod, the ends will be machined and new end plugs are welded to the ends. The length of the finished rodlet specimen will be between 100 and 300 mm, to be decided. The rod will be internally pressurised and then closed by welding, or alternatively connected to a gas supply system for active control of the pressure. The rod is placed in a furnace and heat treated at a specified temperature. The temperature of the sample will be measured using a thermocouple attached to the fuel rod by a clamp. The rod will then be kept in the furnace in the hot cell at constant conditions for a predetermined time to collect creep data.

After creep testing, cooling of the sample can be performed at a predetermined cooling rate or it might be cooled by natural convection. The

test parameters (internal pressure and temperature) can be set as to optimise conditions for hydride re-orientation during the cooling phase.

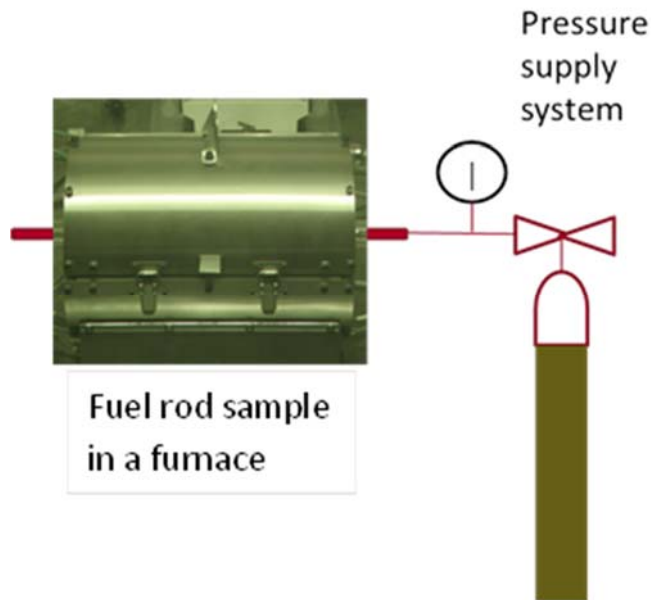


Figure 8

A simple schematic illustration of a possible system for creep testing of fuel rod specimens

Pre-test characterisation

The selected fuel rods will be pre-characterised by profilometry and oxide thickness measurements. The hydrogen concentration in the cladding will be determined and the hydride morphology will be examined by microscopy. The microscopy will also include characterisation of the fuel-cladding bonding layer.

Test matrix

The proposed test matrix for heat treatment under internal pressure is presented in Table 3. The first test would be used to determine what threshold stress is required to achieve cladding lift-off. Subsequent tests are performed at a few constant stress levels below the threshold. The aim is to determine the creep rate and if there is an incubation time before lift-off. Samples from the same fuel rod will also be defueled and creep tested to make direct comparisons between creep curves with and without fuel bonding. Cooling after creep testing will be done slowly under applied internal pressure to allow for hydride re-orientation. A few additional tests at lower stresses of approximately 80-90 MPa may be performed to determine the threshold for hydride reorientation, if this appears to be different than the threshold for defueled cladding.

Table 3

Preliminary test matrix for heat treatment under internal pressure

Material	With/without fuel	Stress [MPa]	Temperature [°C]	Note
PWR, SRA cladding, bonded	With fuel	Ramp	400	Determine threshold for lift-off
PWR, SRA cladding, bonded	Both	200, 130	400	Creep rate, lift-off?
BWR, RXA cladding, bonded	Both	200	400	Creep rate, lift-off?

Post-test examinations

Post-test examinations will include profilometry and microscopy. Microscopy will reveal if any break of the fuel-cladding bonding layer and reopening of the gap has occurred. The hydride morphology after the creep test will be examined. If hydride reorientation has occurred, samples for mechanical testing by the ring compression method will be taken at different locations. The ring compression tests will be used to determine the loss of ductility.

The deliverable will be a report containing test descriptions and results.

2.1.4 Subtask 1.4 – Special fuel rods

Main author: Johan Stjärnsäter

Background

In most countries, the final disposition route of spent nuclear fuel (SNF) is not yet available. Instead intermediate storage solutions are applied on a large scale and becoming increasingly important. Pool storage has been used safely for decades and dry systems are becoming widely implemented. To maintain safe operation and minimise the time, dose and human resources associated with management of SNF, it is important to minimise the amount of damaged fuel. In this context, the principle of classifying a fuel as ‘damaged’ should be based on whether or not the SNF is able to fulfil the required safety, regulatory or operating functions during post-operation, such as handling and storage. This is the definition provided in the IAEA publication [9], which presents management strategies of damaged spent fuel in different countries.

The definition shows that defects, including cladding penetrations, alone are not sufficient to conclude that a rod or assembly is damaged. The defect has to impede the fuel from performing its intended functions. Damaged fuel is fuel that needs non-standard handling to ensure it will perform its required functions.

The required safety, regulatory or operating functions will depend on the planned and potential routes for interim and final disposal of the fuel, which differ from country to country. The functions will translate into characteristics which will determine if the fuel is to be classified as 'damaged' or not.

Cladding breaches have historically been the primary cause for classifying a fuel as damaged. However, other characteristics may also be important, such as characteristics, which may lead to failure of the fuel at a later stage, i.e. during post-operation handling and storage. For long-term interim storage strategies, where it is expected that the SNF will be re-packaged in the future, an important function is the integrity of the fuel cladding during the interim storage period. This function needs to be considered for fuel with characteristics such as high cladding corrosion, thick crud layers, high hydrogen content, hydride blisters, high internal pressure, which may lead to radial hydrides etc. Fuel rods with these characteristics may be considered weak and potentially 'damaged'. Another example is fuel which has been exposed to an anticipated operating occurrence (AOO) or class 3 transient, such as overheating without cladding failure. In SCIP III, it was shown that short-term transient overheating anneals the cladding, which may result in excessive creep and potentially failure of the cladding in dry storage.

Since many SNF management strategies will include transportation at different times, e.g. before and after interim storage, the fuel response to transport vibrations, shocks and accidents needs to be considered. The important functions in this case are the preservation of fuel geometry, and integrity and to inhibit fission product release. As above, fuel rods with characteristics, which may challenge these functions, may be considered weak and potentially 'damaged'.

For utilities, there is a desire to manage the damaged fuel along with the undamaged fuel. However, for utilities with some fuel exhibiting characteristics which may be considered to challenge the post-operation functions, special and costly precautions may be required, such as complete encapsulation. This kind of requirements may be overly conservative and may be challenged using experimental data on fuel rods with the relevant characteristics.

Studsvik disposes of a fuel rod bank that also includes defect rods with cladding breaches, extensive corrosion, hydriding and spalled oxide. Samples from such rods may be used to assess cladding integrity during simulated handling, transport and storage conditions.

To study this phenomenon carefully and to systematically collect data that could support modelling, unirradiated pre-oxidised and hydrogen charged cladding materials might be used in a parametric study.

The subtask will also discuss the fuel rod characteristics criteria applied when classifying a fuel rod as weak or damaged, and which inspection techniques might be suitable to support this classification.

Objectives

- Evaluate and test non-destructive inspection techniques, which may support classification of vulnerable fuel rods.
- Determine mechanical properties of weakened and damaged fuel rods, to establish criteria, which ensure integrity during back-end handling, transport and intermediate storage.

Experimental

The following test methods focusing on fuel rod integrity and cladding ductility will be applied:

- Tensile tests with equipment recently installed in the hot cells on defueled cladding samples and, after modification of the equipment, on fuel rod samples with fuel.
- Ring compression testing of defueled cladding samples and possibly of samples containing fuel.
- Four-point bend tests with equipment installed in the hot cells (see Section 2.1.7 and Figure 12 on page 38 for details). The tests are run at room temperature, normally with a displacement rate of 1 mm/s, while load and displacement of the loading rollers are recorded. The load cell has a maximum capacity of 2200 N, displacement is limited to about 14 mm.

Impact testing and vibration testing may be implemented, if there is a need to verify integrity due to transport vibrations and in hypothetical transport accident conditions.

Pre-test characterisation

The selected fuel rods will be pre-characterised by gamma scan, profilometry and oxide thickness measurements. The hydrogen concentration in the cladding will be determined and the hydride morphology will be examined by microscopy.

Test matrix

The matrix for tests with unirradiated cladding material will be determined later.

The preliminarily proposed test matrix for irradiated material is shown in Table 4. Samples from weak or damaged rods will be tested. The execution of this task and the test matrix will depend on the availability of fuel rod samples.

Post-test examinations

Post-test examinations will include visual inspection and microscopy.

All fractures will be characterised and documented in relation to any anomaly such as oxide spalling, hydrogen blisters etc.

The deliverable will be a report containing test descriptions and results with conclusions.

Table 4

Preliminary test matrix for potentially weakened fuel rods

Material	Burnup [MWd/kgU]	Hydrogen concentration	Tests	Note
PWR, Zircaloy-4	50-60	High	Bend test, RCT, Tensile	Heavy oxidation
BWR, Zircaloy-2	40-60	Very high	Bend test, RCT, Tensile	Very high hydrogen content
BWR or PWR	40-60	Very high	Bend test, RCT, Tensile	Breached cladding, secondary hydriding

2.1.5 Subtask 1.5 – Hydride reorientation

Main author: Kwadwo Kese

Background

Hydride precipitation occurs during operation in the reactor, when the hydrogen solubility limit is reached for the matrix material of the cladding at the temperature involved. The hydrogen comes from oxidation of the cladding by the coolant and from radiolysis of the coolant. The hydride precipitate is in the form of platelets that align themselves in the circumferential direction on a transversal cross section of the cladding [10].

During dry storage and/or transportation, fuel decay heat can cause the cladding temperature to rise to maximum temperatures of up to 400 °C or higher [11]. This rise in temperature will lead the hydride precipitate to dissolve back into solid solution. During subsequent cooling of the spent fuel, hydride re-precipitation occurs depending on factors such as the cooling rate and the hydrogen content. If tangential stresses are present in the cladding during re-precipitation, the hydride orientation tends to be radial on the transverse cross section. Hydride reorientation is then said to have occurred relative to the previous tangential orientation.

Tangential stresses in the cladding could arise from the rod internal gas pressure. In the radial orientation, the hydride could impart brittle behaviour to the cladding under certain load and temperature conditions during storage and transportation [12], with the potential to have a weakening impact on the structural integrity of the used fuel rod. There is therefore the need to understand how the net orientation of the hydride defines the ductile-to-brittle behaviour of the cladding material. Hydride reorientation also depends on factors such as the amount of hydride, hydrogen content, irradiation and cooling temperature. An understanding of these factors will help to predict the ductile-to-brittle transition

temperature (DBTT) during long-term storage. Of particular interest would be the ability to capture the re-orienting crystalline hydride in its nucleation stage in establishing the mechanism of its formation as influenced by grain boundaries, types of precipitate and vacancy or interstitial loops.

Objectives

Against this background, the objective of this subtask is:

To determine the conditions and mechanism for hydride reorientation in irradiated cladding material and, based on the understanding of these parameters, to predict both the hydride reorientation and ductile-to-brittle transition behaviour of the material.

Experimental

Set of experiments 1

Thermal cycling, with applied stress and controlled hydrogen content, will be performed on irradiated and unirradiated specimens to attempt to determine the start of nucleation for radial reorientation of the hydride crystals. Advanced microscopy such as FEG-SEM and TEM will be used to examine the thermally cycled specimens in order to establish the effect of grain boundaries, secondary phases and irradiation damage on the hydride reorientation process.

Set of experiments 2

The next phase of the experimental work will use knowledge from the initial phase to perform experiments on specimens to achieve various degrees of hydride reorientation. The specimens will be mechanically tested at different temperatures and the results used to generate DBTT curves [13]. Sample materials will be selected such that gaps in existing data on DBTT are bridged. Studsvik has in storage a wide variety of candidate materials with different hydrogen content, burnup level and cladding material. This provides an excellent opportunity for SCIP IV to complement DBTT data obtained previously and fill some of the existing data gaps.

Test Matrix

The following test matrix is proposed (Table 5) for the hydride reorientation experiments where H1, H2, and H3 represent different hydrogen contents.

Table 5

Proposed schedule for hydride reorientation tests

Material	Burnup [GWd/tU]	Hydrogen [ppm]	Temperature [°C]	Hoop stress [MPa]
BWR, Optimised ZIRLO	50	H1	250-400	70-150
	55	H2		
	60	H3		

2.1.6 Subtask 1.6 – Delayed hydride failure during interim storage

Main author: Anna-Maria Alvarez

Background

Until recently, research on fuel cladding integrity has been focused on performance during reactor operation. In view of extended interim storage periods, more emphasis is put into understanding of fuel performance under these conditions. Consequently, the temperature range of experimental studies needs to be expanded from 400 °C down to about 150 °C.

It is well known that sensitivity to hydride induced failures in Zirconium alloys increases at lower temperatures. Two types of hydride induced failure mechanisms have been observed in zirconium alloys; one that acts on the macroscopic scale, and one that acts locally, in front of a stress concentrator. The first one is classical hydride embrittlement (HE), which occurs instantaneously on a macroscopic level, once the applied stress exceeds the fracture stress of a highly hydrided component [14] [15] [16] [17]. Extensive studies show that there is a ductile to brittle transition (DBT) that depends mainly on temperature, hydride concentration and hydride reorientation. HE under back end conditions will be studied in Subtasks 1.4 and 1.5, where the DBT will be determined in samples with dense hydride lenses and/or radially oriented hydrides.

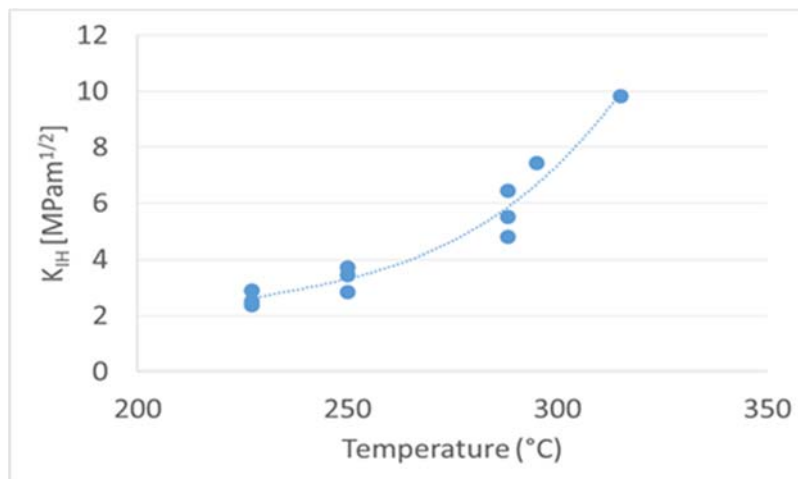
The second mechanism, delayed hydrogen cracking (DHC), is a time-dependent mechanism that acts on a local level in front of stress concentrators. It operates at much lower macroscopic hydrogen and stress levels than classical hydride embrittlement and is therefore relevant for all fuel rods. Four critical parameters for DHC to operate in a fuel rod are listed in Table 6.

Table 6

Values of the critical parameters for DHC, as observed in out-of pile tests observed in previous studies

Critical parameter	Value	Ref.
Minimum hydrogen concentration C_H [wppm]	$C_{TSSP} < C_{Hcrit} < C_{TSSD}$	[18] [19] [20] [21]
A temperature below the maximum temperature, T_{max} [°C]	≈350-385 °C (high burnup ZIRLO)	[22]
Sufficient time for through wall cracking or minimum crack velocity V_{DHC} [m/s]	$v_{(DHC)} = 2 \cdot 10^{-7} - 5 \cdot 10^{-7}$ at 300 °C	[23] [24] [25]
Stress intensity above threshold, K_{IH} [MPa√m]	4-12	[26] [27] [28] [29] [30] [31]

All four parameters have to be fulfilled simultaneously for the mechanism to occur. The three first parameters (hydrogen concentration, temperature and time) are all fulfilled for most rods during back end handling. But the mechanism will not operate, if the fourth parameter, the critical stress intensity for DHC initiation (K_{IH}), is not exceeded. A precise value of K_{IH} is therefore crucial for predicting DHC failure during back end handling. The K_{IH} for unirradiated Zircaloy-4 as a function of temperature has previously been studied within a Coordinated Research Project (CRP) round robin organised by the International Atomic Energy Agency [32]. Some of the results from Studvik are shown in Figure 9. One can see that K_{IH} decreases with temperature. The lowest value for K_{IH} was observed at 227 °C and was determined to be 2.6 MPa√m.

**Figure 9**

Threshold stress intensity factor as a function of temperature for unirradiated Zircaloy-4 fuel cladding

In order to initiate a DHC crack, the combination of tensile stress and flaw size must exceed K_{IH} . Assuming the value of K_{IH} applies to a radial

crack, the maximum depth of sharp surface flaw, a , that can be tolerated without crack growth can be estimated according to [33]:

$$a = (K_{IH}/\sigma)^2 \times Q/1.2\pi$$

with σ = applied stress and Q = shape factor

For elliptical flaws, Q is about 1.5, while for long flaws, Q is about 1.0.

During dry storage of spent LWR fuel, a hoop stress is imposed by internal pressure. Applying the U.S.NRC limit of 90 MPa, [34] and [35] suggest that the critical flaw size for DHC at 227 °C is 221-332 μm , if K_{IH} is 2.6 $\text{MPa}\sqrt{\text{m}}$, dependent on crack geometry. Since neutron irradiation may reduce K_{IH} [36], it is important to establish K_{IH} in irradiated fuel as well as to narrow down the scatter to obtain a more precise value of K_{IH} .

Objectives

There are two main objectives of this subtask:

- To determine K_{IH} for irradiated fuel cladding in the temperature range 150-400°C. Based on the results, critical (maximum) length of flaws in the cladding will be determined at internal pressures relevant under back end conditions.
- To study the effect of impact/bending on DHC, by performing bending or impact tests on fuel rods with hydride lenses and/or radial hydrides followed by a constant load.

Experimental

Determination of K_{IH} in irradiated fuel cladding

It is proposed that the pin-Loading tension (PLT) technique, developed to study DHC [31], is used in the tests. The configuration of the PLT specimen and fixture is shown in Figure 10. The PLT fixture consists of two halves, which form a cylindrical holder when they are placed together. The cylindrical holder has a diameter that allows it to be inserted into the tubular PLT specimen. The fixture halves are loaded in tension through pins at **A** and rotated around pin **B**. Before starting the test, the specimen should be fatigue pre-cracked to produce a sharp crack of about 1.5 mm in front of the machined notch **C**. During the DHC test, the specimen should be heated to 385 °C for 60 minutes to dissolve most of the hydrides, with a low load on the specimen. The sample is then cooled with no undercooling to the test temperature. After 30 min, load is applied to a maximum K_I of 15 $\text{MPa}\sqrt{\text{m}}$, where load is held constant until the crack starts to propagate. During the test, crack propagation is measured continuously with the Direct Current Potential Drop (DCPD) technique. Once the crack has grown a certain length, the load is reduced and the process repeated until no cracking is detected for 24 hours. This value of

K_{I} represents the threshold value, K_{IH} . A typical test curve from the DHC PLT tests is shown in Figure 11.

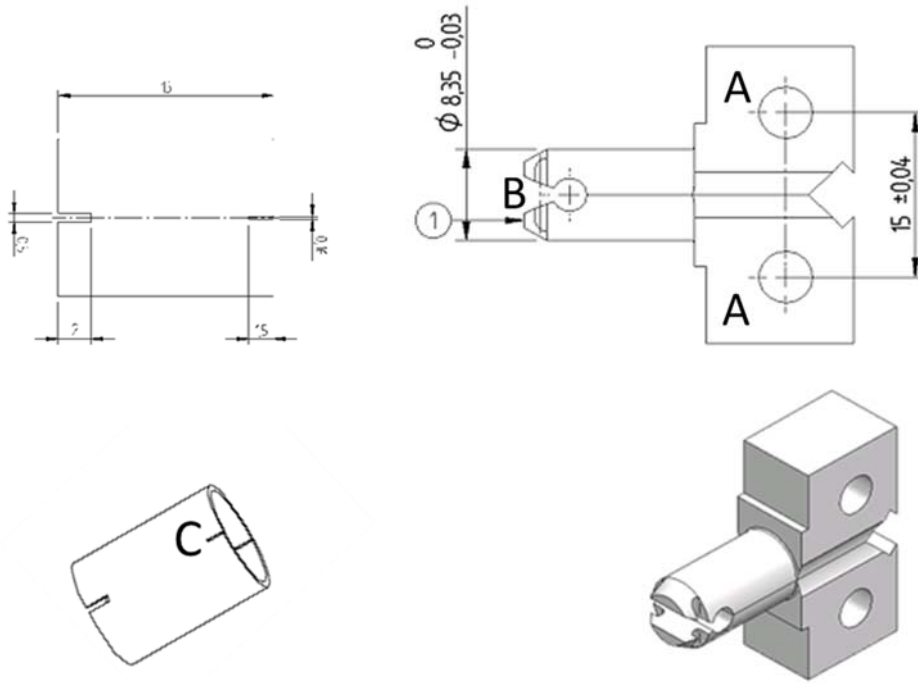


Figure 10
 Schematics of PLT specimen (left) and fixture (right)

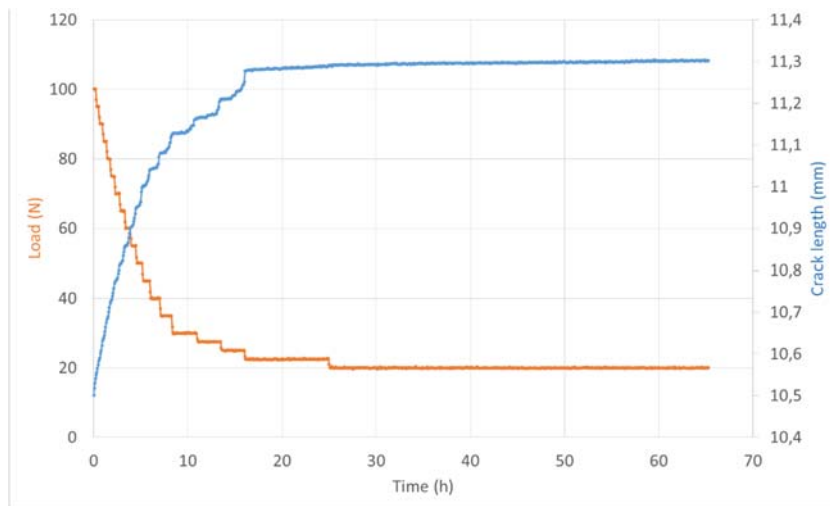


Figure 11
 A typical diagram from a PLT test at 227 °C, where load and crack length are plotted versus time

Effect of prior impact/bending on the initiation of DHC in fuel cladding

As mentioned above, DHC does not operate without an initial flaw or stress concentrator in the fuel cladding. For most spent fuel, no flaw of critical size is expected in the fuel cladding wall at end of life. It is not

expected either that it will be introduced during normal transportation and handling. If, however, a high burnup PWR cladding of the older generation is subjected to a drop or bending, hydride dense areas may crack and cause a non-through wall crack. This may serve as an initiation site for DHC. To investigate the effect of rod drop or bending on DHC during intermediate storage, it is proposed that integral tests are performed, where rods with or without fuel are tested with four-point bend or internal pressure, followed by a constant load (90 and 120 MPa) at constant temperature of 150-250 °C.

Proposed test matrix

It is proposed that Zircaloy-4 is used, since this alloy has been extensively studied and the material data and mechanical properties of this alloy are well known. Furthermore, this material has an extensive hydrogen uptake and it is therefore more likely that incipient cracks in oxide or hydride rim will form during a drop. For the K_{IH} measurements, we propose a maximum burnup level of 45 MWd/kgU, since it would be difficult to spot weld the DCPD wires to highly oxidized fuel cladding. For the combined simulated drop case + DHC studies, it is proposed to use high burnup samples.

Table 7
Proposed test matrix

Material	Burnup [MWd/kgU]	Type of tests	Temperature [°C]
Zircaloy-4	20-45	PLT K_{IH} determination Stepwise load reduction	150-400
Zircaloy-4	45-70	Four point bend /internal pressure Fast load followed by constant load at 90 and 120 MPa	150-250

Post-test examinations

After the PLT tests, the fracture surfaces will be examined in the light optical microscope to measure the length and geometry of the machined notch, fatigued incipient crack and DHC crack. Some samples will also be characterised by SEM to confirm that the crack propagated by means of delayed hydride cracking. In the combined tests, where bending has been followed by constant load, fractography and selected cross sections will be performed, in order to identify initiation site, incipient cracks in hydride lenses and/or radial hydrides and crack propagation mechanism.

2.1.7 Subtask 1.7 – Spent fuel rods in transport and handling operations and in accident scenarios

Main author: Joakim Karlsson

Background

After having reached end-of-life burnup, spent nuclear fuel (SNF) is stored in the spent fuel pool. The fuel is cooled down over at least several months and more likely over several years. The fuel is then put into intermediate storage, which could be an on- or off-site dry storage system or wet storage facility. In this process, SNF is handled, loaded and transported and unloaded and/or stored. The exact sequence of transportation and storage depends on the system employed, which differs between countries and facilities. Many years later, when a final storage solution is available, the fuel may need to be transported and handled again to prepare and encapsulate it for its final resting.

A very large number of SNF transports have been performed successfully worldwide. Only for special transportation conditions or accident situations is there a substantial need to verify SNF behaviour and suitability for further storage. One example is the study of fuel rods' resistance to vibrations during rail transport, as investigated by the U.S.NRC at Oak Ridge National Laboratory (ORNL) [37]. The tests were performed using a Cyclic Integrated Reversible-bending Fatigue Tester (CIRFT) system developed to test and evaluate the mechanical behaviour of spent nuclear fuel. The studies show that the margin to failure by vibration fatigue is very large. Only if a fuel rod sample is exposed to an impact shock prior to vibration fatigue testing, there is a significant reduction of the fatigue resistance.

Another case where normal SNF transport needs to be verified is for weak, damaged or failed fuel rods. Examples are excessive secondary hydriding after a pin-hole failure, excessive cladding corrosion and hydride blistering. In such cases, the fuel may be considered damaged or weak. Without data to verify the strength of such fuel rods, special and costly precautions may be required by authorities, such as complete in-pool encapsulation, before the fuel can be moved out of the SFP. This kind of requirements may be overly conservative.

For organisations with multiple reactors, some plants may shut down earlier than others. If the reactors use the same fuel design, there is an economic incentive to reuse fuel, which has not been fully burnt. The fuel could be taken from a closed plant and transported to another plant, which continues to operate. A transport between the two plants will include handling operations, cask loading, movement by road or rail and then cask unloading and reuse. This will involve movement of the SNF from vertical to horizontal and back. It is important to verify that these operations do not adversely affect the fuel. For example, the spring may have relaxed due to irradiation and by moving the SNF from vertical position to horizontal and back it is important not to create gaps in the fuel

pellet stack, which may result in cladding collapse. Another issue is vibration during transportation and the risk of dislodging and moving pellet fragments and thereby creating local stress concentrations, which may result in fuel failure during subsequent irradiation.

For accident conditions, the fuel rod response needs to be experimentally verified and there is limited data available. As can be cited from [38], “It should be noted that the data from mechanical tests with cladding tensile specimens or with empty tube specimens give generally a limited benefit in this context because of different behaviour of fuel rods as a composite structure of cladding and spent fuel. Bending tests with axial segments of irradiated fuelled rods are more useful for clarification of these questions but such experimental data are hardly available now for public use.”

One of few examples is the fuel integrity project of BNFL and TNI, where six static bending tests with irradiated fuel rod specimens were carried out [39]. Compression tests were also performed of empty tube segments [40]. The results provided data for analytical models of fuel rod bending in a 9 m lateral regulatory drop. Although the test program was publicly reported, only a limited part of the experimental data was disclosed. Furthermore, practically no information was provided on the fuel rods, e.g. information on cladding material, dimensions, oxide thickness and hydrogen content and its morphology. This severely limits the usability of this work.

Studies of fuel break under impact loads have been performed at ITU and reported in [41] and [42]. These tests used fuel at several burnups and they showed very limited mass of less than two grams of fuel released per rod break. Despite these tests, there is still lack of detailed data on the respirable fraction of high burnup fuel fragments, which may be released in high energy impact events involving transport casks. Such data are available for low burnup fuel [43] and have been requested by the U.S.NRC for high burnup fuel [44].

The discussion above shows that there is very limited experimental data available on fuel rod response under transport accident conditions. This is valid both for mechanical data such as bending and compression tests of irradiated fuel rods and for detailed data on respirable fractions of fuel fragments.

Objectives

The first objective is to generate valuable experimental data on the mechanical response of irradiated fuel rods under transport accident conditions. The purpose of the data is in turn to support analytical models for regulatory accident evaluation. Apart from transport accidents, the data produced will also be useful for seismic and vibratory evaluations.

The second objective is to characterise the particulates which might be released from high burnup fuel rods due to impact events. The results

will support cask containment analysis and the definition of source terms for accident scenarios.

The third objective is to investigate the potential effects of handling and transportation of low burnup fuel and verify its safe reuse after transportation.

The final objective is to study the strength of weak or slightly damaged fuel rods under transportation and handling operations. The aim is to verify that weak or slightly damaged rods will not degrade or jeopardise cask safety functions during transportation and storage.

Experimental

The most valid method to test response of fuel rods under accident conditions is to perform bend tests. Bending test equipment available in the Studsvik hot cells is shown in Figure 12 (left). The machine was originally built and used in the U.S.NRC LOCA test program [45]. It is based on a modified Instron™ machine. Tests are run at room temperature with a pre-determined displacement rate of usually 1 mm/s, while the load and displacement of the loading rollers are being measured. The load cell has a capacity of 2200 N and the maximum useful displacement is about 14 mm.

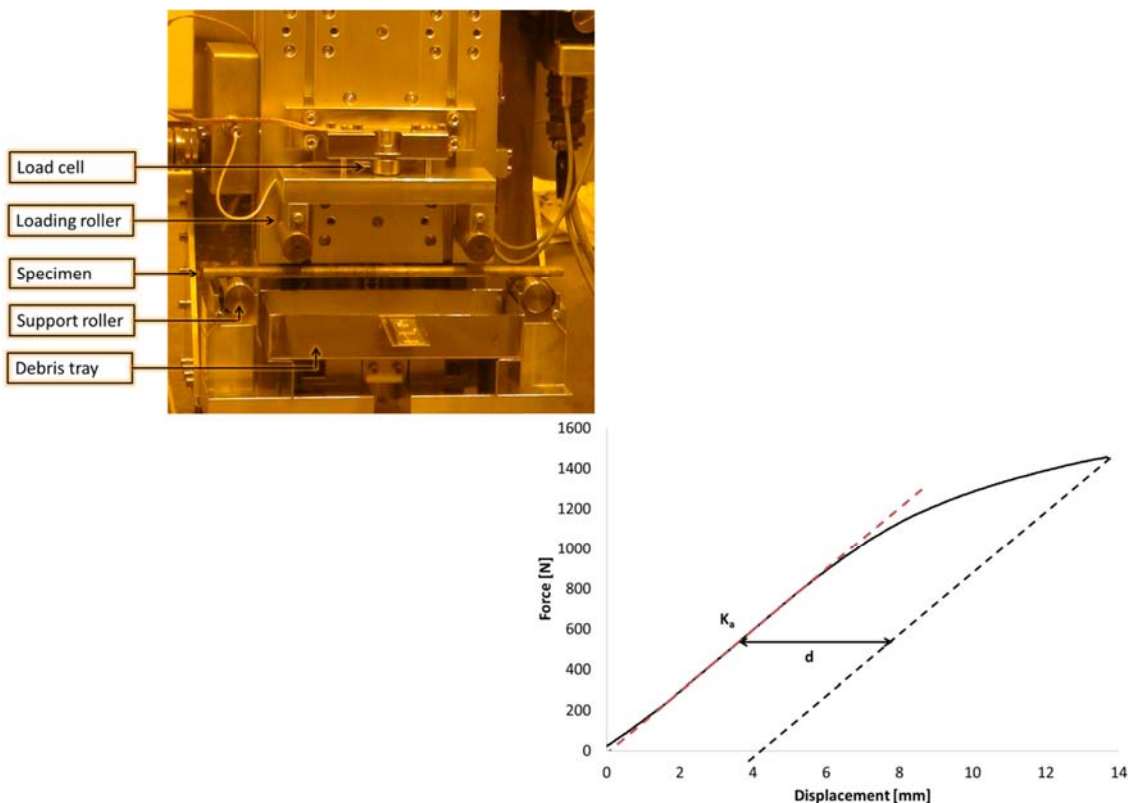


Figure 12

The 4-point bending machine in the hot cell (left) and measured force vs. displacement curve for an unirradiated verification specimen (right)

The test data in Figure 12 (right) show the result from a bend test on an unirradiated empty cladding tube of Zircaloy-4. The slope of the deflection curve in the elastic regime is given by $P_a = K_a \delta_a$, where P_a is the load measured by the load cell in response to the controlled displacement δ_a measured by the machine actuator. The slope K_a in Figure 12 (right) is related to the bending stiffness EI of the specimen by the equation

$$K_a = \frac{12EI}{a^2(3L - 4a)}$$

where L is the distance between the two supports and a is the distance between each loading roller and the closest support. For irradiated fuel rods the bending stiffness increases mainly due to bonding between fuel pellet and cladding. For a brittle irradiated fuel rod the rod may fail in the test and in this case the plastic bend deformation to failure is obtained. The unirradiated cladding tube providing the results shown in Figure 12 (right) was ductile and it did not fail. Total plastic bend deformation d was obtained as indicated in the plot. Data from bend tests are important for modelling fuel behaviour in transportation accidents or in seismic events. For example, measured values of the bending stiffness of fuel rods can be used to determine realistic critical inertia load magnitude values for fuel rod buckling in transportation accidents [46]. When brittle irradiated fuel rods break in the bend test, fuel fragments are ejected. By weighing the dispersed fuel fragments, fuel loss can be quantified. Further characterisation may be performed by SEM and by particle counting and size determination.

Another method, which will be used to characterise the sample materials is ring compression testing. Ring compression on samples with fuel inside will provide mechanical properties for fuel and cladding composite material. Such data will support structural mechanical modelling of the fuel rod response in regulatory cask accidents.

In transportation accidents, a drop of the cask will cause a direct impact load on the fuel assembly and the fuel rods. An impact testing device for fuel rods can be used to obtain direct information on the consequences for the fuel integrity from different impact loads. There is no impact testing device currently available at the hot cells, but if desired, impact test equipment can be designed and built as part of this subtask.

Pre-test characterisation

The selected fuel rods will be pre-characterised by gamma scan, profilometry and oxide thickness measurements. The hydrogen concentration in the cladding will be determined and the hydride morphology will be examined by microscopy.

Test matrix

The proposed test matrix is shown in Table 8. Prototypical and representative fuel rods with different burnup will be tested and charac-

terised. In addition, some rods, which are considered weak or damaged will be tested.

Table 8

Preliminary test matrix for fuel rods in transport and storage under normal and accident conditions

Material	Burnup [MWd/kgU]	Hydrogen conc.	Tests	Note
PWR, SRA cladding	45, 65	Low, medium, high	Bend test, RCT, ~Impact	Representative rod
BWR, RXA cladding	45	Low, medium, high	Bend test, RCT, ~Impact	Representative rod
PWR	-	Medium- high	Bend test, RCT	Weak rod. Thick oxide. Hydride blisters
PWR or BWR	-	High	Bend test, RCT	Weak rod. Secondary hydriding

To verify the reusability of low burnup fuel rods, it is proposed that a suitable rod will be characterised and subjected to handling and orientation changes. Post-test characterisation will then verify the condition of the fuel rod and the absence of any degradation. Handling operations should be conservative relative to the envelope of accelerations, which a rod is exposed to under handling and transportation. Irradiation induced relaxation of the plenum spring may also be determined for a suitable fuel rod candidate. The purpose is to determine which internal hold-down force remains to keep pellets in place under handling and transportation.

Post-test examinations

Post-test examinations will include visual inspection, gamma scan and microscopy.

Fuel fragments from rods fractured in the tests will be collected and weighed. Further characterisation will include sieving, SEM and particle counting and size determinations.

The deliverable will be a report containing test descriptions and results with conclusions.

2.1.8 Subtask 1.8 – Failed fuel

Main authors: Kyle Johnson, Joakim Karlsson

Background

After having reached its end of life, spent nuclear fuel is typically removed from the plant spent fuel pool. The fuel is transported to a centralised wet storage or put in dry storage casks and placed at a dry storage facility. However, fuel assemblies containing damaged or failed fuel rods

can typically not be handled in the same manner as intact fuel. There are several reasons for this, one is the difficulty to license a cask for transporting failed fuel assemblies and rods, another is the difficulty and risk associated with handling of the damaged fuel in the pool. Furthermore, there is typically no standard route available for final disposition of the failed fuel rods. For example, breached fuel pins have been deemed unacceptable for final storage in the Swedish final repository solution KBS-3, due to the tendency of pre-oxidised fuel matrices to release radionuclides to groundwater at an accelerated rate compared to UO_2 [47]. All this has led operating power plants to slowly accumulate inventories of failed fuel in their respective spent fuel pools.

The storage of failed rods on-site may also be associated with undesirable consequences, such as release of fission products to the pool water. The release also contributes to radioactive waste generation from pool water filtration. The accumulated storage of failed fuel in the pool represents a liability and a contribution to the risk profile of the spent fuel pool.

For plants, which enter a decommissioning process, the removal of the site fissile inventory is a very important first step. This permits the site license to be downgraded, thereby providing a significant reduction in operational costs. This is also a prerequisite to begin physical decommissioning activities. However, the presence of failed fuel pins on site is an issue if these cannot be readily transferred to either intermediate or final storage sites.

For safe long-term stabilisation of failed fuel the radiological confinement needs to be restored and the geometry and environment needs to be controlled and stable. There are different concepts available to encapsulate damaged and failed fuel rods either by canning in-pool or by conditioning and encapsulation at a hot cell. In Sweden, Studsvik has been able to provide this important service by transporting and receiving inventories of failed fuel at its hot cell facility, perform conditioning, and encapsulation for compatibility with the existing final storage solution in Sweden.

Drying of failed fuel is essential to avoid gas generation by radiolysis of residual water and moisture. Availability of oxygen and hydrogen gas in the container could have undesirable consequences, such as oxidation of the fuel, hydriding of the cladding, corrosion and pressure build-up in the container [48]. The removal of residual water and moisture presents a significant challenge for the safe removal and long-term stabilisation of failed fuel, since the failed rods may be completely filled with water. Many failed fuel rods have also been water-logged for up to 30 years and water has had ample time to access and fill all tiny cracks and open volumes in the fuel rod.

The importance of residual water in dry storage cask systems has been investigated to some extent by industry and regulatory organisations [49]. As a result of this work, an ASTM standard has been developed [50]. The

standard provides guidance as to the drying of intact spent nuclear fuel in dry storage casks. However, for failed fuel the standard drying procedure may not be sufficient to guarantee the required moisture level for encapsulation of failed fuel. It can be concluded that test methods to measure moisture content need to be developed and validated to prove that criteria on moisture content can be met. Furthermore, available drying procedures need to be evaluated for failed fuel and possibly optimised.

Objectives

The objective of the subtask will be to generate experimental data on the issue of safe encapsulation and storage of failed fuel rods using PIE characterisation methods and assessment of residual water.

Experimental

Sections of irradiated and water-logged fuel will be dried and different techniques will be employed to evaluate and locate any presence of moisture adsorbed on fuel and clad surfaces, as well as any moisture present inside the fuel rod. The main technique will be thermal gravimetric analyses, but other techniques may also be applied.

To determine the effectiveness of the drying procedures applied, the moisture content before and after drying will be compared.

Test material

This task will utilise fuel rods, which have failed during in-reactor operation and then been transported to the Studsvik hot cell for PIE. Fuel from intact fuel rods may also be soaked and dried in the tests.

2.2 Task 2 Loss-of-coolant accidents

2.2.1 Subtask 2.1 – Microstructure related to fuel fragmentation

Main author: Anders Puranen

Background

The existence of a burnup threshold with regards to fuel fragmentation in LOCA scenarios has been a key question in several studies and research efforts such as in the Halden reactor program, the EPRI and U.S.NRC sponsored Studsvik tests, in SCIP III and elsewhere. As the experimental evidence grows, it seems that fine fragmentation does not readily occur for fuels with a pellet average burnup below ~60-65 MWd/kgU. High burnup by itself however only appears to be one factor, several tests have shown that fuels with considerably higher burnup, up to the 75 MWd/kgU range appear to resist fine fragmentation under similar conditions as in which a susceptible fuel with a burnup around 65 MWd/kgU undergoes severe fragmentation. Several hypotheses have been brought forward to explain this behaviour, such as effects of the power history inducing residual stresses in the pellet, or repartitioning of

the fission gas inventory to closed grain boundary networks or bubble populations that weakens the integrity of the fuel under a LOCA event. Recent results from SCIP III [51], [52], [53] have identified the potentially very important effect of microstructural transformation leading to sub-grain formation ... (*SCIP III proprietary information deleted*).

In order to study this potentially important phenomenon further, we propose to continue on the advanced microscopy examinations performed in SCIP III on fuels with high burnup that fragment to a large extent in LOCA like conditions, as well as to study high burnup fuel that appears resistant to fine fragmentation.

Experimental

The main method to quantify the degree of sub-grain formation is SEM-EBDS. LA-ICP-MS may also be employed to investigate the actual fission gas content of fuels both pre- and post-testing. This may include post-test analysis of fine fragments to determine their radial origin; in order to improve the statistics, automated image analysis may be employed for this task. Grain boundary oxidation or fuel annealing with online measurement of released fission gas may also be employed to determine the role of induced fission gas release in the fine fragmentation process. Additional heating tests or LOCA tests may be performed to challenge and verify the outcome of the microscopy investigations.

2.2.2 Subtask 2.2 – Fuel fragmentation, relocation and dispersal in non-standard fuel

Main authors: Hans-Urs Zwicky, Per Magnusson

Background

“Standard fuel”

In SCIP III, investigations on FFRD focused on the performance of “standard fuel”, i.e. UO₂ fuel with an as-fabricated grain size in the order of 10-15 μm. Numerous heating tests and a selection of LOCA tests revealed that there does not exist a simple burnup threshold for FFRD. The degree of FFRD is not simply dependent on last cycle power either. Instead, it was found that fuel behaviour during heating and LOCA tests depends on the pre-test fuel microstructure that has developed in the course of operation. Detailed investigations of fuel samples irradiated to high burnup demonstrated that microstructure is strongly dependent on the entire local power history, potentially leading to completely different structure at the same burnup. As explained in Section 2.2.1, microstructural transformation leading to sub-grain formation also beyond the rim region might be very important.

Large grain, doped and additive fuel

Already in the early days of commercial nuclear energy production, attempts were made to influence material properties of UO_2 fuel by adding dopants, in order to reduce fission gas release and swelling during irradiation. Two basic approaches were studied. By adding aliovalent dopants, it was tried to alter the diffusion of the fission gases by adjusting the defect structure of UO_2 . As an alternative, dopants were studied that led to larger grains, thus increasing the diffusion path. An example of such a study, with chromia (Cr_2O_3) as a grain growth promoter, was published in [54]. As chromium is a trivalent additive, it was furthermore thought that the fuel would be sub-stoichiometric, which could lead to a reduced rare gas diffusion coefficient. Results of comparative tests with Cr_2O_3 doped and pure UO_2 samples with an initial grain size of 50-55 and 6 μm , respectively, but the same density did not at all reflect the expectations. Fission gas release and swelling were roughly the same. Nevertheless, detailed examination of the samples revealed some important findings. The observed fission gas release could only be explained satisfactorily, if an enhanced rare gas diffusion coefficient and a reduced grain boundary surface energy were assumed. Grain boundary porosity developed differently in the two fuel types as well.

This and other studies' ambiguous results were probably not the main reasons why the concept of fuel dopants was not pursued aggressively. Instead, performance of pure UO_2 fuel fabricated under controlled industrial conditions became well predictable. This, in combination with appropriate fuel rod mechanical designs, allowed limiting the consequences of fission gas release and fuel swelling. The situation changed when utilities started to increase their demands on fuel regarding manoeuvrability, power and burnup. This brought FGR and PCI back into the focus of fuel manufacturers.

After comprehensive screening studies and extensive testing, AREVA chose 0.16 wt% pure chromia as a dopant. The grain size is typically in the order of 50 μm (linear intercept method). High density, in the order of 10.63 g/cm^3 (97 % theoretical density), can easily be achieved. High density improves thermal conductivity, which leads to lower maximum fuel temperature. Chromia does not impact neutron absorption too much. Chromia doped fuel is now a mature product that is supplied in reload quantities in AREVA's most advanced BWR and PWR fuel assembly designs [55].

Westinghouse identified a synergy effect, when testing a combination of chromia and alumina. When adding some alumina, the desired grain size could be reached with much less chromia than without alumina. This is an advantage, e.g. because Cr has a larger thermal neutron capture cross section than Al. As a result of the Westinghouse additive fuel project, ADOPT (**A**dvanced **D**oped **P**ellet **T**echnology) was introduced after extensive testing [56]. ADOPT fuel contains about 700 ppm Cr_2O_3 and 200 ppm Al_2O_3 . The grain size is in the order of 30-35 μm (linear inter-

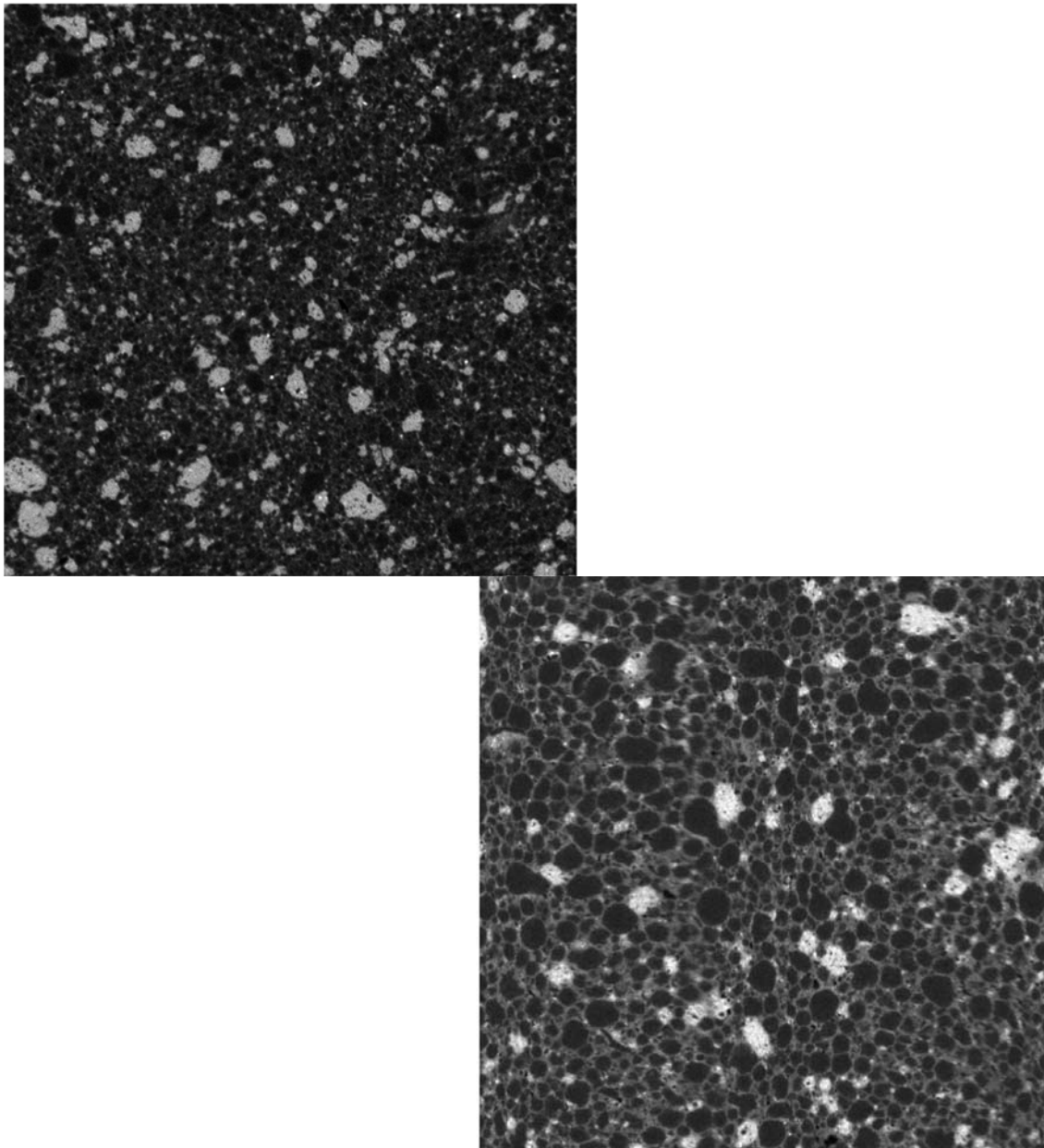
cept method) and the density 10.67 g/cm^3 (97.4 % of theoretical density). Today, ADOPT is the standard Westinghouse fuel supplied in reload quantities and verified to high burnup.

GNF and its associated vendor companies have been developing additive fuel for over 35 years [57]. Development has concentrated on aluminosilicate additives which are virtually insoluble in UO_2 and are present as a continuous intergranular glassy phase thus facilitating grain boundary sliding and producing a compliant or “soft” pellet. The additives employed are either synthetic mixtures of alumina and silica or natural mineral clays, kaolinite with a $\text{SiO}_2/\text{Al}_2\text{O}_3$ weight ratio of about 55:45 and bentonite with a $\text{SiO}_2/\text{Al}_2\text{O}_3$ weight ratio of about 82:18. GNF additive fuel has been successfully irradiated in power reactors since 1977, first in low power segmented rod bundles up to 25 MWd/kgU and later as lead test assemblies achieving more than 40 MWd/kgU and lead use assemblies irradiated to about 20 MWd/kgU before unloading for further testing. In contrast to AREVA and Westinghouse, GNF did not yet introduce additive fuel pellets as commercial fuel in reload quantities.

Independent from the details of the concept chosen by different fuel suppliers, the as-fabricated microstructure of large grain fuel differs from “standard” fuel. Consequently, it might well develop differently during operation as well. As a consequence, fuel performance during a LOCA, in particular with respect to FFRD, may also be different from the fuel investigated so far within SCIP III.

MOX fuel

Uranium-plutonium mixed oxide fuel (MOX) is far from being a homogeneous mixture of UO_2 and PuO_2 [58]. The as-fabricated homogeneity depends strongly on the fabrication process. In the MIMAS (MICronised MASTer blend) fabrication process, pure PuO_2 , UO_2 and recycled (U, Pu) O_2 scrap are first milled to a master blend containing at least 25 % plutonium. In a second step, the master blend is further diluted and milled with pure UO_2 to the target plutonium content, before pelletizing, sintering and grinding. Plutonium distribution and microstructure also depend on the type of UO_2 powder. In MIMAS MOX fabricated with UO_2 precipitated from ammonium uranocarbonate (AUC process), the main portion of plutonium is still found in lumps of master blend, up to some tens of micrometres in size (Figure 13, left). If the UO_2 powder is precipitated from ammonium diuranate (ADU process), the plutonium distribution is more complex. In addition to agglomerates rich in plutonium and uranium, respectively, a “coating phase” is observed with a plutonium content of 4-12 % (Figure 13, right). Almost 50 % of all plutonium is found in this “coating phase”.

**Figure 13**

Electron probe microanalysis, plutonium distribution in as-fabricated MIMAS MOX fuel pellet; UO₂ powder from AUC (left) and ADU (right) process [58]

As a consequence of varying plutonium content, fission density and thus local burnup is much higher in plutonium rich agglomerates. These agglomerates develop a highly porous microstructure, as illustrated in Figure 14. The size of the bubbles increases slowly with burnup and rapidly with temperature, whereas the bubble density decreases correspondingly.

Outside a central zone, where the temperature is lower than about 1000 °C, subdivision of grains occurs in plutonium rich areas, leading to

the same structure as the high burnup rim structure in UO_2 fuel (Figure 15).

Fission gas release in MOX rods is somewhat higher towards high burnup, compared to UO_2 operated under similar conditions. The main reason for this effect is a somewhat lower thermal conductivity of MOX, leading to higher centreline temperature and higher release of fission gases from the pellet centre.

Overall, the microstructure of high burnup MOX fuel is significantly different from the structure of “standard fuel”. As long as the mechanisms leading to FFRD are not thoroughly understood, it cannot be predicted whether MOX fuel fragments less or more during a LOCA. On the other hand, studying MOX fuel behaviour in heating and LOCA tests might well contribute to a better understanding of the mechanisms of concern.

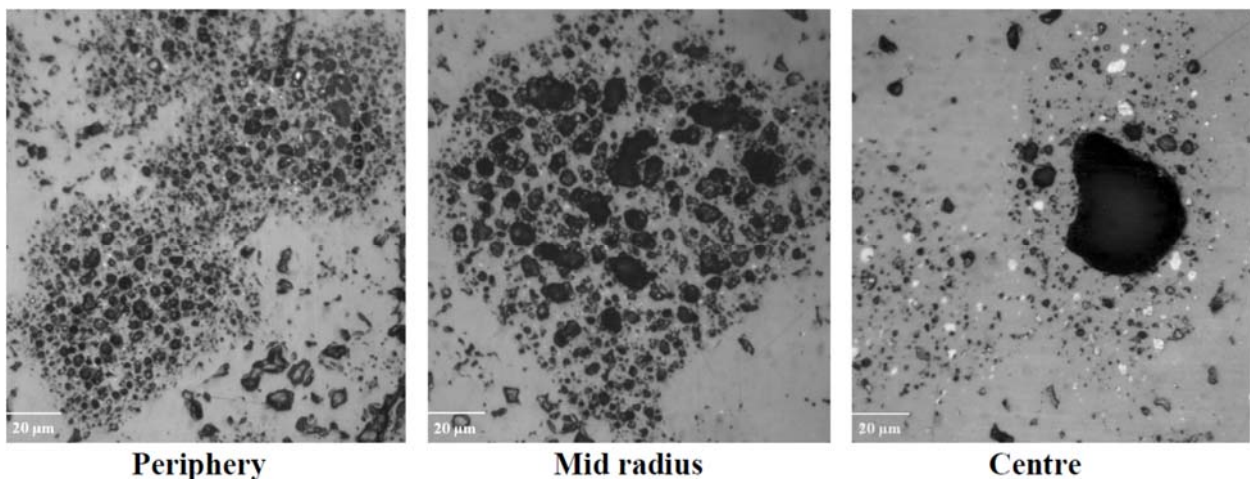


Figure 14
Optical micrograph of Pu rich agglomerates in MIMAS AUC MOX, burnup 55 MWd/kgHM [59]

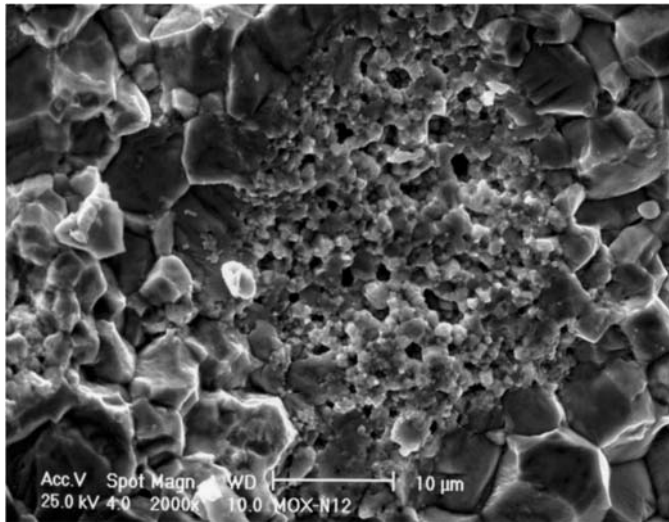


Figure 15
Fractography of agglomerate after 3 annual cycles of irradiation [59]

Gadolinia fuel

One of several options to suppress excess reactivity in fresh fuel is adding gadolinia (Gd_2O_3) to UO_2 . In BWRs, in the order of 10% of all fuel rods contain gadolinia. The gadolinia content is about 5 wt.%, but not higher than 10 wt.%.

Gadolinia can form a solid solution in UO_2 , but production of homogeneous (U, Gd) oxide would require precipitation from correspondingly composed aqueous solutions. In industrial nuclear fuel production, gadolinia and UO_2 powder is blended and milled, before pressing and sintering pellets. Thus, such a burnable absorber fuel pellet normally contains areas with elevated gadolinium content with an extension of up to some tens of micrometres. Physical properties like thermal conductivity, specific heat capacity, thermal diffusivity and expansion of gadolinia pellets are rather close to the corresponding properties of pure UO_2 fuel. Nevertheless, high burnup gadolinia fuel might well perform differently with respect to FFRD under LOCA conditions.

Objectives

Work to be performed under this Subtask aims at extending data base and understanding of FFRD to fuel types that have not yet been investigated within SCIP III or elsewhere. The data will support estimates of fuel dispersal in LOCA safety assessments carried out by utilities and regulators, as well as refinement and extension of fuel fragmentation models to be incorporated in fuel performance and transient codes.

The objectives of the Subtask are the following:

- Determine fine fragmentation burnup threshold for large grain, doped and additive fuel, for MOX fuel and for gadolinia fuel and compare it to the performance of standard fuel

- Determine the dependence of fragmentation on temperature for non-standard fuel types mentioned above
- Investigate relations between burnup and temperature dependence of fragmentation and pre-test fuel microstructure
- Confirm the influence of cladding strain on FFRD for non-standard fuel types

Experimental

Heating tests

Unrestrained heating tests, as described in [60] and performed within SCIP III, are the method of choice to determine burnup thresholds for fine fragmentation and to study the dependence of fine fragmentation on temperature.

Fuel heating tests are performed in a radiant tube furnace installed in a hot cell. The furnace has three 80 mm long individually controlled heating zones. A 500 mm long quartz tube with a diameter of 30 mm is used. Fuel samples are tested under ambient air atmosphere, typically up to a temperature around 1000 °C. The sample temperature is directly recorded by a thermocouple attached on the sample. Fast heating rates, typically in the order of 10 °C/s, can be obtained by preheating the furnace to the target temperature, before inserting the sample. Figure 16 shows the furnace set-up, installed inside a hot cell. These tests are normally documented by means of a video camera (visible on the left side of Figure 16), which also records the sound emitted from the sample, when it is heated. A typical temperature – time curve is shown in Figure 17. The sample constraint is removed by cutting an axial slit through the cladding. In this way the fuel is basically intact with minimum damage from sample preparation.

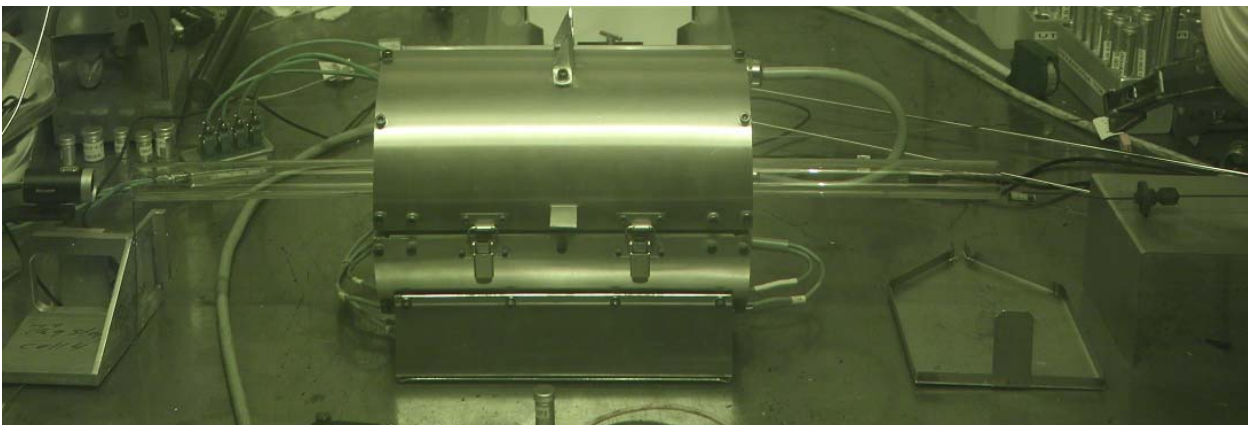


Figure 16
Furnace used for fuel heating tests installed in hot cell

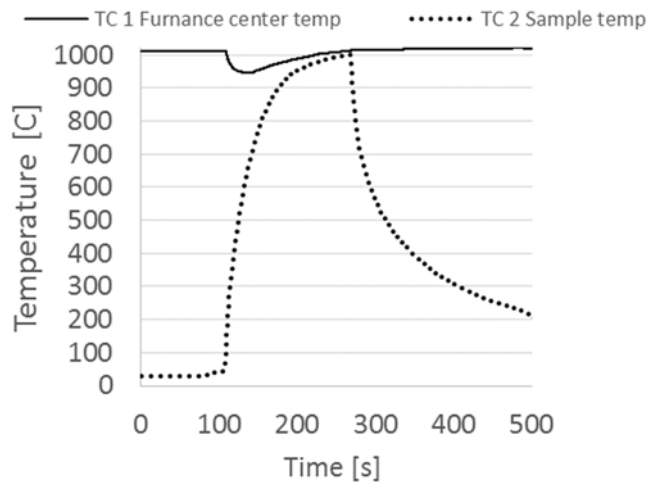


Figure 17
Plot of furnace and sample temperature versus time, recorded in a typical fuel heating test

The scope of the heating test matrix depends on the available budget. It will include

- Samples with varying burnup, but basically the same power history, from the same fuel rod, cut at different elevations
- Samples with similar fuel types and comparable burnup, but from rods with different power histories
- Samples with all non-standard fuel types mentioned above, as far as they can be made available at reasonable cost

LOCA tests

Based on the heating test results and within budget limits, a series of out-of-pile LOCA tests will be performed, in order to confirm trends established by heating tests and the influence of cladding strain on FFRD for non-standard fuel types.

Studsvik operates two integral LOCA test rigs. The first rig was built on behalf of the U.S. NRC to perform the same type of LOCA testing as earlier done at the Argonne National Laboratory [61]. The second LOCA test device, which is planned to be used in SCIP IV, is a development of the first rig with increased performance and test capabilities.

The apparatus is designed to externally heat an up to 40 cm long fuel segment up to 1200 °C by infrared (IR) radiation. The test segment temperature is measured with a thermocouple attached on the rod approximately 50 mm above the axial mid plane. The test segment is pressurized with helium or argon and placed in a quartz glass chamber in a flowing steam environment, air or inert gas (argon) atmosphere. It is also possible to combine different environments such as an air-steam mixture to simu-

late LOCA scenarios in a spent fuel pool. The main parts of the apparatus are sketched in Figure 18. A pressure transducer placed in the plenum above the specimens measures the rod inner pressure. The transient steps are fully controllable, which allows for testing of all types of time-temperature transients, heating rates, cooling rates, number of temperature steps, quench temperature, etc. The test environment and rod inner pressure are set at the start of the transient. The axial elongation of the specimen is measured during the test by means of a Linear Variable Differential Transformer (LVDT). It is also possible to apply axial load to the specimen at any time during the transient. In a typical integral LOCA test, the fuel segment is internally pressurized to 50 – 100 bar and heated with a 5 °C/s ramp. At 650 – 800 °C, the rod balloons at mid-height and ruptures. Heating continues to 1100 – 1200 °C, where the temperature is held for a predetermined time. Afterwards, the rod is cooled down to a preselected quench temperature, typically at 700 – 800 °C, before the test chamber is flooded with room temperature water.

After the test, the segment may be characterised by techniques such as profilometry, 4-point bending, gamma scanning, etc. The fuel loss can be determined and the oxidation of the cladding may be evaluated by means of metallographic examinations. The content of hydrogen in the cladding can be analysed, e.g. with hot vacuum extraction (HVE). Post-test characterisation provides information on, amongst others, cladding strain, ballooning and burst, fuel fragmentation, cladding oxidation, hydrogen pickup, and transient fission gas release. Rod inner pressure and cladding outer temperature are recorded during the test.

Axial temperature profiles at different temperatures and stream conditions were determined during commissioning tests. The profile at 1200 °C is shown in Figure 19. Technical details of the device can be found in [62] and [63].

The specifications of the LOCA test device are as follows:

- Axial load up to 1000 N
- Axial displacement measured online
- Rod internal pressure up to 20 MPa, online logging
- Temperature of specimen up to 1200 °C
- Environment control (steam, air, steam and air, argon)
- Quench
- Collection of dispersed fragments for analysis.
- Fully controlled transient, with controlled heating and cooling rates

Microscopy

Pre- and post-test samples will be characterised by means of advanced microscopy and, if necessary, related investigating techniques like EPMA and laser ablation combined with ICP-MS.

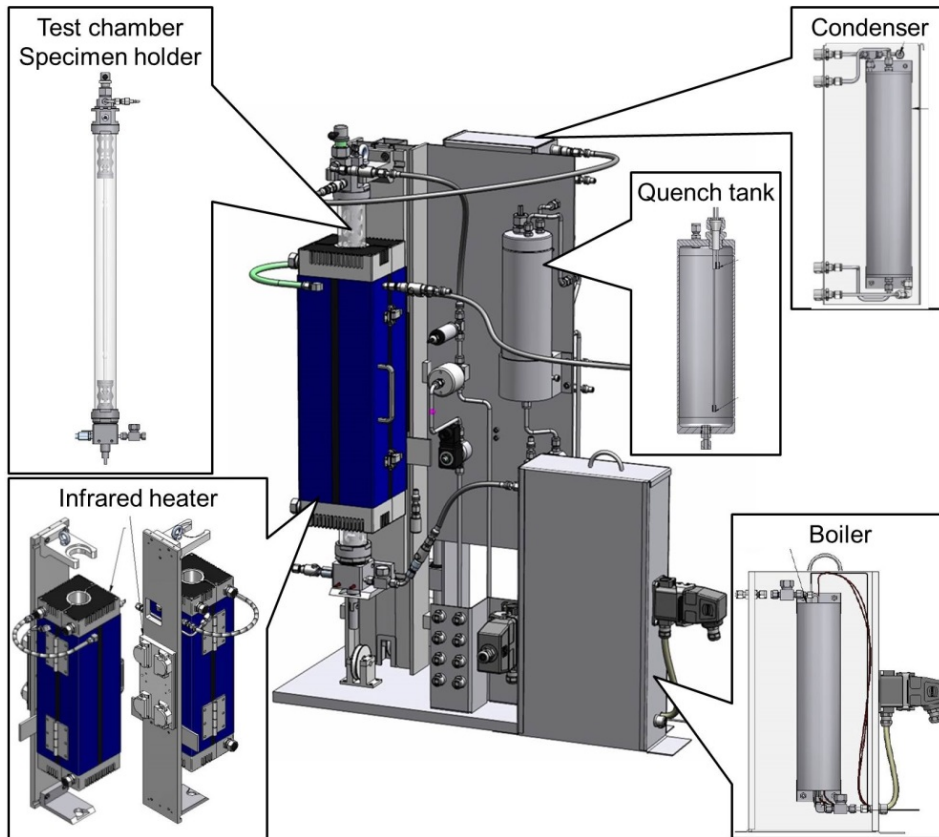


Figure 18
 Front view of the LOCA apparatus showing the main parts

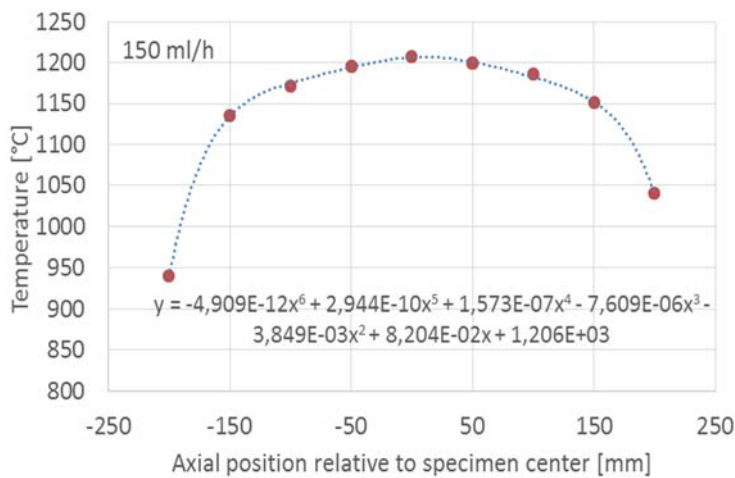


Figure 19
 Axial temperature profile of the IR furnace in the new LOCA rig at 1200 °C

2.2.3 Subtask 2.3 – Separate effects tests

Main author: Anders Puranen

Background

In order to improve the understanding of fuel fragmentation in LOCA scenarios, a number of separate effects test are suggested regarding the temperature and depressurisation transient that a fuel rod undergoes in a LOCA event leading to a burst. The tests in SCIP III have indicated that for fuels susceptible to fine fragmentation critical parameters may be both the temperature ramp rate and the magnitude of the depressurisation transient upon burst. The temperature ramp rate experiments in subtask 1.1 of SCIP III using the heating test furnace have evidenced a strong correlation between increased degree of fine fuel fragmentation with increasing heating rates, although a slow heating ramp integral LOCA test of a fuel known to be susceptible to fragmentation still led to severe fragmentation [64], [65]. The degree of temperature ramp rate control of the heating test furnace used in these tests is however limited since the furnace heater is of a resistive type, only enabling temperature ramp profiles rather dissimilar to those expected in a LOCA transient. The construction of a new furnace with infrared heating enabling fine control of the temperature profile similar to the LOCA testing device is therefore proposed, to more accurately investigate temperature ramp rate effects. The new furnace would still be substantially less intricate than the LOCA testing device, enabling tests with short fuel specimens at lower cost and complexity than in the larger LOCA testing device.

With regards to the impact of the depressurisation transient upon burst on the degree of fine fragmentation, a small set of LOCA tests has been performed in SCIP III [66], indicating a strong effect of the burst pressure. Interestingly, the fuel fragmentation in a LOCA transient might share mechanisms with one of the most destructive classes of volcanoes, the pyroclastic eruptions [67]. We therefore propose to perform burst depressurisation tests on fuel susceptible to fragmentation in a way similar to which geologists have extensively studied the phenomenon of fine fragmentation of rock with highly pressurised pores. In the case of pyroclastic events, magma rises quickly from the deep high pressure interior of the earth, while it cools and solidifies in a strong pressure gradient. This leads to formation of highly pressurised porosity that causes the rock to undergo brittle fragmentation as it nears the surface, leading to massive eruptions of hot ash plumes. These phenomena have been extensively studied by pressurising volcanic rock with a high degree of open porosity in a chamber fitted with a burst disk, enabling well controlled and rapid depressurisation transients. This has shown that rock fragmentation occurs by brittle failure with a strong correlation between the pressure differential and the porosity of the rock [68]. High speed photography has also shown the propagation of a depressurisation and fragmentation shockwave from the burst location into the material [69]. Although the

rock morphology and mechanical properties are quite different from high burnup fuel, the basic phenomena might be very similar to a LOCA rod burst event. In the LOCA case we therefore hypothesise that fine fuel fragmentation might be facilitated both by the high-pressure fission gas inclusions that form during irradiation, and possibly by the gas pressure in cracks and open porosity that would depend on the pressure of the rod at time of burst. The degree of fragmentation might therefore depend strongly on the rod pressure and the rate of depressurisation, causing a fragmentation shockwave that attenuates in the fuel column away from the burst opening in a LOCA transient. This effect might explain the observed correlations with higher degrees of fine fragmentation in the rod sections nearer to the burst opening and with higher diametrical cladding strain (loss of restraint and facilitation of gas movement). Post-test examinations of LOCA tested rods from both Studsvik and Halden have also indicated that the fragmentation can stop rather abruptly at pellet-pellet interfaces, with a pellet closer to the burst opening being severely fragmented and the next seemingly unaffected. This might prove to be related to the dampening of a propagating shock wave initiated by the depressurisation at pellet interfaces.

In summary, we propose that a new furnace is constructed to better control the temperature ramp rate in tests of similar size as the existing heating test apparatus (testing a few pellets worth of material) and that the equipment is made compatible with a new depressurisation rig being able to simulate the burst event with high degree of control, including an expansion chamber to contain and collect the ejected fuel fragments for further study. Once critical parameters have been identified, a few integral LOCA tests might be performed to verify the results.

Experimental

A new infrared furnace similar to the one in the LOCA device [62] will be used. The furnace might be positioned vertically to facilitate collection of fragments ejected during heating tests. The equipment will have the option to flow gas through it (such as argon).

The depressurisation equipment would consist of a cylindrical pressure vessel with a means to affix one end of the fuel specimen inside. The cylinder inner diameter would be slightly larger than the fuel section to also accommodate fuel samples with an axial slit similar to those used in the heating tests of SCIP III. The fuelled portion would fit inside the furnace. The depressurisation would be controlled by selection of different burst disks depending on desired burst pressure. The burst disk would be fitted at the end of the cylindrical pressure vessel connected to a pressure resistant transport tube connected to an expansion chamber outside the furnace from which the expelled fuel fragments could be collected. Depending on the scope, the expansion chamber could be made gas tight and evacuated to less than atmospheric pressure and have the means to

collect a gas sample after the burst, in order to quantify any fission gas release from the tests.

The minimum post-test examinations scope would consist of photos of the specimens as well as weighting and sieving to determine the extent of fuel fragmentation. Additional examinations such as collection of released fission gas for FGR calculations and post-test microscopy may be applied on selected samples. Advanced microscopy such as SEM to examine fracture surfaces and LA-ICP-MS to examine the remaining fission gas content or fuel fragment oxidation tests for fission gas release may also be employed (see Section 2.2.1).

2.2.4 Subtask 2.4 – Fuel and cladding oxidation in LOCA

Main author: Alexandre Barreiro

Background

Effect of pre-transient corrosion

One of the main concerns in a large break LOCA regarding the zirconium alloy cladding failure is the oxidation of the alloy itself, which results in embrittlement and fracture of the cladding[70]. Among several possible detrimental consequences derived from this event, the generated steam can also get into contact with the fuel through the fractured cladding, leading to oxidation of the fuel surface.

Cladding embrittlement is well studied [70] and several correlations exist for oxidation kinetics [71][72][73][74][75][76] and oxygen-stabilized alpha layer growth under LOCA conditions [72]. However, most of these studies have been performed with unirradiated material. CEA studies on high temperature steam oxidation of unirradiated zirconium based nuclear fuel claddings revealed that pre-corroded samples inside an autoclave at 340-360°C showed weight gains lower than those of uncorroded materials, when exposed to the same conditions for short oxidation times (1-3 minutes at 1200 °C), and similar weight gains for oxidation times longer than 8 minutes [77]. The results show no protective effect of the pre-transient oxide layer on post-quench mechanical properties of the cladding. However, less pre-transient corrosion could still have a positive effect, simply because the load bearing area of the cladding wall is larger.

A pending issue is to demonstrate the applicability of results acquired with unirradiated material on irradiated cladding. Results from LOCA tests performed in SCIP III that focused on the impact of high temperature steam oxidation on mechanical properties of the cladding indicated that corrosion performance might be influenced by the pre-test oxide layer. These data will form the starting point for more detailed studies within SCIP IV, consisting of high temperature oxidation tests with fuel rod samples with and without fuel, followed by corresponding post-test characterisation, in order to compare performance of irradiated cladding

with unirradiated material tested under the same conditions. In addition, potential oxygen uptake from the irradiated fuel can be assessed.

Effect of steam pressure

During a small break LOCA, oxidation of Zircaloy can occur at high pressure, whereas most steam oxidation tests reported in the literature have been carried out at atmospheric pressure. As observed by [78] and more recently by [79], pressure can enhance oxidation. The most relevant results have been reported by [80], where it was demonstrated that oxide layer thickness and pressure were directly correlated. Several authors have provided a consistent series of results revealing the pressure effect upon the oxidation kinetics at temperatures between 750-1000 °C. However, all these tests have been performed on unirradiated material. Data on temperatures higher than 1000 °C are also lacking. SCIP IV will study high temperature oxidation on irradiated cladding at different steam pressures by means of new test equipment. The results will support establishing a correlation to calculate ECR values at steam conditions relevant for small break LOCAs.

Fuel oxidation

If a fuel rod bursts after a small break LOCA, the fuel will be exposed to steam and/or water and radionuclides might be released into the plant's system. Exposure to steam and/or water will lead to oxidation of uranium increasing its solubility and the release of radionuclides to the system. Understanding this process will help to assess the radiological status of the plant after a small break LOCA.

Fuel fragmentation is caused by cracking during normal operation inside a reactor. During LOCA transients, the fuel is further fragmented, in particular at high burnup, as demonstrated by in-pile and out-of-pile LOCA tests and in heating tests.

SCIP IV will characterise fragmented fuel by means of XRD, in order to identify oxidised uranium oxide phases such as U_3O_8 . The results will be compared to pre-test irradiated fuel and to as-fabricated fuel crushed under inert atmosphere at room temperature.

Additionally, WDS could be applied on samples of irradiated fuel from LOCA tests that did not lead to severe fragmentation, to compare oxygen profiles and profiles of potentially volatile fission products. The results would be compared to maps from pre-test samples.

One possibility would be to build a dedicated oxidation device that is smaller and simpler than a LOCA device to oxidise both cladding and fuel pellets.

Objectives

The main objectives of this subtask are to investigate the following parameters:

- Cladding oxidation:
 - Study the consequences, if any, of in-service corrosion on subsequent high temperature oxidation of cladding during a hypothetical HT LOCA transient, using irradiated zirconium based claddings. The behaviour will be compared to pre-corroded unirradiated zirconium based cladding performance.
 - Study the effects of in-service corrosion and hydriding on post-quench ductility by using irradiated cladding and comparing the results to unirradiated analogues reported in literature.
 - Study the effect of pressure during HT steam oxidation of irradiated zirconium based cladding at pressures higher than 0.1 MPa and compare it to the behaviour of unirradiated pre-oxidized claddings found in the literature.
- Fuel oxidation:
 - Study the fragmented fuel by means of XRD to detect, if formed, more oxidized phases such as U_3O_8 . The results will be compared to those from pre-test and as-fabricated samples.
 - Study oxygen profiles in fuel pellets that did not exhibit severe fragmentation by means of WDS. Fission product profiles will also be studied.
 - Perform oxidation tests with dedicated equipment on single pellets with cladding.

Experimental*Pre-test characterisation*

Pre-test examinations of the selected fuel rods will include profilometry and oxide thickness measurements. The hydrogen concentration in the cladding will be determined and the hydride morphology will be examined by microscopy.

XRD and WDS studies will be performed on the pre-test and as-fabricated samples

Oxidation

Tests will be performed both on defueled cladding and on short fuel segments. The test material will be taken from fuel rods with relevant in-

service corrosion irradiated in power reactors. Temperature and steam conditions will be chosen to allow for comparison with results from non-irradiated material.

A new oxidation device will be designed and built that allows for variable steam pressures and the possibility to oxidise short fuel segments (single pellets with cladding).

Post-test examinations

Post-test examinations will include profilometry, oxide thickness measurements and microscopy. Alpha and prior-beta layers of the cladding wall will also be measured.

XRD and WDS studies will be performed on the post-test samples.

2.2.5 Subtask 2.5 – Spent fuel pool LOCA

Main authors: Pia Tejlund, Hans-Urs Zwicky

Background

Loss of coolant in a spent fuel pool (SFP), with high temperature oxidation of cladding in an air-steam mixture as well as transients leading to ballooning and burst of fuel rods, can have severe consequences.

Within SCIP III, only two LOCA tests under simulated spent fuel pool conditions have been performed. Moreover, the scope of post-test examinations was rather limited. Therefore, additional SFP LOCA tests, covering a broader band of potential conditions, will be performed in SCIP IV. The scope of post-test examinations will be extended, providing additional data to define the fission product source term for this type of events.

Objectives

The objectives of the Subtask are the following:

- Extend the knowledge base on cladding corrosion and fuel rod performance during and after transients in air-steam mixtures, as they might occur in spent fuel pool LOCA events
- Provide data to define the fission product source term for loss-of-coolant accidents in spent fuel pools

Experimental

LOCA tests

Studsvik operates two integral LOCA test rigs. The newest LOCA rig planned for use in SCIP IV is described in Section 2.2.2 on page 50. In this Subtask, the test environment will be an air-steam mixture prototypical for conditions that might occur during a spent fuel pool LOCA. The

fuel rod segments will undergo LOCA transients including ballooning and burst. The effluents from the tests will be collected for analysing fission products.

The scope of the test matrix depends on the availability of budget and suitable fuel rods. It will include samples with different cladding types and burnup values.

Sample characterisation

In addition to the usual pre- and post-test examinations (visual inspection, oxide layer thickness, profilometry, gamma scanning, metallography and ceramography), samples taken from the father rod and from the tested fuel rod will be investigated with advanced examination techniques, including, amongst others, Scanning Electron Microscopy combined with wavelength dispersive X-ray spectroscopy and laser ablation combined with Inductively Coupled Plasma Mass Spectrometry, in order to assess changes in the content and distribution of fission products.

2.2.6 Subtask 2.6 – Post LOCA seismic loads

Main author: Per Magnusson

Background

Post-LOCA seismic loads have been identified as a potential accident scenario that could challenge core coolability and safety of a nuclear power plant [81]. In a seismic event the fuel assemblies could be impacted by lateral movements and vibrations, causing bending and cyclic loads on the fuel rods [82]. If the fuel properties have already been degraded during a LOCA, the risk of failure due to seismic loads is increased. In a LOCA transient, where fuel rods are exposed to steam at very high temperatures, the cladding will suffer degradation of its mechanical strength due to several mechanisms. Extensive oxidation and spalling will decrease the cladding thickness and hydriding will embrittle the cladding. Another mechanism which contributes to cladding embrittlement is the change in cladding microstructure by formation of an oxygen stabilized alpha layer. Since oxygen is an alpha stabilizer, a transformation of the high temperature beta zirconium into alpha zirconium occurs when a sufficiently high oxygen concentration is reached in the cladding. This will occur in the region close to the zirconium oxide, leading to an alpha layer beneath the oxide. Cladding embrittlement then occurs because oxygen-stabilised alpha zirconium is more brittle than beta zirconium.

The mechanical properties of the fuel rod are also likely to have been degraded by normal operation in the reactor. As burnup increases so do amount of corrosion, neutron irradiation dose and absorbed hydrogen. If the fuel rods break due to seismic loads and degraded mechanical properties, fission products, fuel fragments and cladding pieces would be released into the coolant flow channel and the coolable geometry of the

reactor core could be impaired. A good understanding of the seismic loads that may be imposed on the fuel rods and a good evaluation of the resistance of the fuel rods to such loads are therefore vital to ensure the safety of LWRs after a loss-of-coolant scenario. Cladding resistance to embrittlement after a LOCA transient has been studied by methods such as ring compression tests, ring tensile tests, four-point bend tests and integral LOCA tests with axial load [83]. To evaluate post-LOCA seismic loads, four-point bend tests have the advantage that also ruptured cladding can be tested. Evaluation of post-LOCA mechanical properties by four-point bend tests has been reported in several studies. [84][85]. A comprehensive study on fuel rod resistance to post-LOCA seismic loads using non-irradiated material was performed by JAEA [84]. It found that the resistance of ruptured fuel to seismic bending moments depends on the pre-transient hydrogen content for intermediate ECR of 10 to 20 %. At higher ECR the resistance was completely determined by the oxidation time. Furthermore, the study found that cyclic loads did not significantly deteriorate the fuel rod mechanical properties. To compare the results with actual fuel, several factors should be considered, such as annealing of irradiation hardening, fuel bonding, and how the fuel column affects the stress distribution in the cladding.

In SCIP III, a device for integral LOCA tests has been developed that is able to study fuel rod resistance to axial loads after ballooning, burst and high temperature oxidations (see Section 2.2.2 and Figure 18 on page 52). The results were used to evaluate fuel rod resistance to axial loads during quench (so called thermal shock tests) and to compare with previous results on defueled cladding tubes and non-irradiated material. The device also has the capability to apply post-transient axial loads. The same device can be used to produce specimens for seismic load experiments. Fuel rod segments will be subjected to LOCA transients including balloon, burst, high temperature oxidation and quench. Afterwards, the segments will be tested by 4-point bend tests or by axial load tests to determine which loads would compromise coolability in a post-LOCA seismic event.

Several factors influence the mechanical resistance of the fuel rods to seismic loads:

- Oxidation (time and temperature) of the cladding during the LOCA transient
- Hydridding of the cladding during the LOCA transient
- Heating rate, cooling rates and quench temperature during the LOCA transient
- Irradiation, hydridding and corrosion of the cladding prior to the LOCA transient
- Bending moments and cyclic loads caused by seismic motions

Material and transient conditions need be chosen in a way that allows determining fuel rod seismic failure limits and comparing results with literature data on non-irradiated material.

Objectives

The objective of this subtask is to evaluate fuel rod resistance to post-LOCA seismic loads:

- Bending moment to failure of fuel rod segments with different pre-transient characteristics and ECR levels
- Impact of cyclic loading of ductility and failure moment

The gathered data will support estimates of fuel rod resistance to seismic loads in LOCA safety assessments carried out by utilities and regulators. Moreover, they will indicate, how representative data on non-irradiated and on defueled material are, compared to rods with fuel.

Experimental

The proposed work of this subtask can thus be summarized as:

- Modification of the 4-point bending device to allow for cyclic loading.
- A series of integral LOCA tests on fuelled rod segments to different oxidation and hydrogen content levels.
- Testing of these segments by 4-point bend tests, cyclic 4-point bend loads, and axial loads.
- Evaluation of test data and assessment of the seismic load resistance. Comparison with literature data from tests with defueled cladding tubes and non-irradiated material.

The scope of the test matrix depends on the available budget. It will include:

- Fuel rod segments with varying pre-transient conditions; burnup, corrosion level and hydrogen contents.
- Different transient conditions in form of oxidation time and temperature.
- Different post-LOCA load tests:
 - 4-point bend tests to determine maximum bending moments
 - Cyclic loading prior to failure tests to determine how/if cyclic deflection will change the rod mechanical properties.
 - Cyclic load tests until failure.

- The samples will be taken from standard commercial LWR fuel rods, as far as they can be made available.

LOCA Tests

Studsvik operates two integral LOCA test rigs. The newest LOCA rig planned for use in SCIP IV is described in Section 2.2.2 on page 50. In this Subtask, the test segment is pressurised with helium or argon and placed in a quartz glass chamber with a flowing steam environment. The fuel rod segments will undergo LOCA transients including ballooning and burst as well high temperature oxidation to different ECR levels. After LOCA testing, the fuel rod segments will be used for post-LOCA seismic load tests.

4-point bending tests

The 4-point bending machine planned to be used for the experiments in this Subtask is described in Section 2.1.7 on page 38. For SCIP IV, it is proposed to modify the equipment to allow for controlled cyclic loads.

Pre-test characterisation

The selected fuel rod segments will be pre-characterised by profilometry and oxide thickness measurements. The hydrogen concentration in the cladding will be determined and the hydride morphology will be examined by microscopy. Microscopy will also include characterisation of the fuel-clad bonding layer.

2.2.7 Subtask 2.7 – Transient fission gas release and axial gas communication

Main author: Per Magnusson

Background

During a loss-of-coolant accident (LOCA), rapid and large changes of temperature may cause transient fission gas release (TFGR) from the fuel, by mechanisms such as fuel grain boundary fracture or diffusion and interconnection of fission gas bubbles. Understanding of the transient fission gas behaviour is important to determine factors such as increase in rod inner pressure and margins to cladding burst and loss of rod integrity. Knowledge of the transient fission gas release also allows for a more accurate determination of the source term in an accident scenario. Several TFGR studies have been performed by annealing of small fuel pieces [86], or in some cases single pellets [87][88] or short fuel columns [89]. Integral LOCA tests have also been performed to study transient fission gas release in [90] and in SCIP III. The results of these studies showed a trend of increased transient fission gas release with burnup. However, the scatter in the results was considerable.

The two main mechanisms leading to transient fission gas release are grain boundary fracture occurring at lower temperatures, and diffusion

activated at higher temperatures (>1000 °C). If grain boundary fracture is the main release mechanism, it can be assumed that larger transient fission gas release occurs in higher burnup fuel due to a higher amount of fission gas in grain boundary bubbles. In annealing studies performed on very small fuel pieces high fission gas release was observed, when the pieces fragmented [86]. Rim fragmentation is hence also a possible contributor to increased transient fission gas release. To further assess transient fission gas release, it is proposed to perform a parametric study by means of modified heating test equipment, using fuel rod pieces with a length of a few centimetres. The advantage of using this method, compared to integral LOCA tests, is that a larger number of tests can be performed to study effects such as burnup, peak temperature and holding time. The results can then be verified and benchmarked against dedicated integral LOCA tests.

In order to properly assess the effects of transient fission gas release on local pressure and ballooning and burst, it is important to know the axial gas communication inside the fuel rod. In SCIP III, studies of axial gas communication were performed on four fuel rod segments. The measurements were performed either at room temperature or at 300 °C. To further extend the knowledge base on fuel permeability and gas communication under transient conditions, it is proposed to perform a parametric study of axial gas communication against burnup and temperature. The results will support improving fuel performance code models of gas communication under transient conditions.

Objectives

The objective of this subtask is to evaluate transient fission gas release and axial gas communication inside the fuel rods.

- Transient fission gas release as a function of burnup
- Transient fission gas release as a function of temperature
- Transient fission gas release as a function of hold time
- Axial gas communication as a function of burnup
- Axial gas communication as a function of temperature

The data will support calculations of transient fission gas release and axial gas communication in transient conditions. The results will support better estimations of fuel rod local pressure, which will improve knowledge of the margins to cladding burst and loss of rod integrity. The transient fission gas release data will also allow for a more accurate determination of the source term in accident scenarios.

Experimental

The scope of the test matrix depends on the available budget. It will include:

- TFGR heating tests of fuel rod segments with varying burnup
- TFGR heating tests with different peak temperatures and hold times
- Integral LOCA TFGR tests to benchmark and verify heating tests results
- Measurement of axial gas-communication at transient temperatures
- Pre-characterization of fuel rod segments to be tested

LOCA Tests

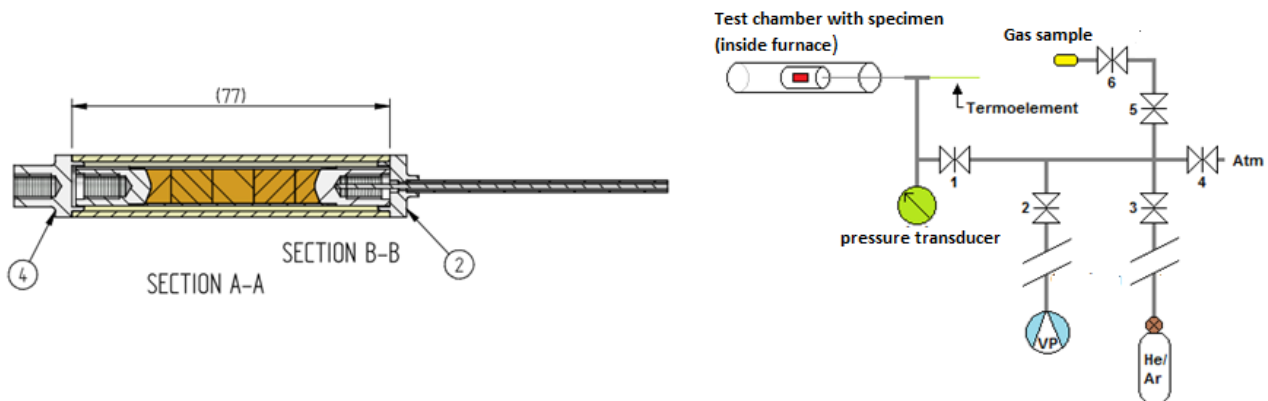
Studsвик operates two integral LOCA test rigs. The newest LOCA rig planned for use in SCIP IV is described in Section 2.2.2 on page 50. The device allows collecting fission gases from the specimen after the transient through a valve in the plenum. The collected fission gas samples can be analysed by an InProcess Instruments GAM-400 gas mass spectrometer.

Heating tests

Unrestrained heating tests have been performed in SCIP III to determine burnup thresholds for fine fragmentation and to study the dependence of fine fragmentation on temperature. The fuel heating tests are performed in a radiant tube furnace installed in a hot cell. The furnace has three 80 mm long individually controlled heating zones. A 500 mm long quartz tube with a diameter of 30 mm is used. Fuel samples are tested in air under ambient pressure, typically up to a temperature around 1150 °C. The sample temperature is directly recorded by a thermocouple attached on the sample. Fast heating rates, typically in the order of 10 °C/s, can be obtained by preheating the furnace to the target temperature, before inserting the sample. A modified heating test setup is proposed for SCIP IV experiments.

Pre-test characterisation

The selected fuel rods segments will be pre-characterised by gamma-scanning and light optical microscopy. Microscopy will include characterisation of the fuel-cladding gap or the bonding layer as well as fuel microstructure and porosity.

**Figure 20**

Modified heating test device for measurements of transient fission gas

2.3 Task 3 – Pellet-cladding interaction

2.3.1 Subtask 3.1 – Data for modelling

Main author: Joakim Karlsson

Background

Fuel performance codes use different methods and criteria to determine when a PCI failure occurs. Examples of such failure criteria are cladding peak stress, cumulative damage index (CDI) and strain-energy density (SED). Each method has its pros and cons as was presented and discussed in the SCIP II MWS ([91], [92] and [93]).

The CDI method has the advantage of being based on out-of-pile SCC data. It takes both the time dependence and the chemical environment into account. Data for standard Zircaloy-2 and Zircaloy-4 cladding have been available for many years [94]. An example of PCI failure data published in 1980 is shown in Figure 21 [95]. However, there is little or no data on more modern cladding materials, for example radial texture Zircaloy-2 with liner and the Nb-containing PWR claddings such as ZIRLO™ and M5™.

Studsvik has equipment and experience for performing creep measurements under constant stress and temperature on cladding tube specimens. There is also a lot of experience from mandrel testing regarding the handling of Iodine.

In this subtask the aim is to obtain SCC time-to-failure data for irradiated cladding tubes of modern materials. The data will also be evaluated, compared to existing old data and put into a form suitable for use in fuel performance codes. Model calculations can then be performed and the damage predictions with the new dataset can be compared to those based on the old set and also be applied to the SCIP ramp tests.

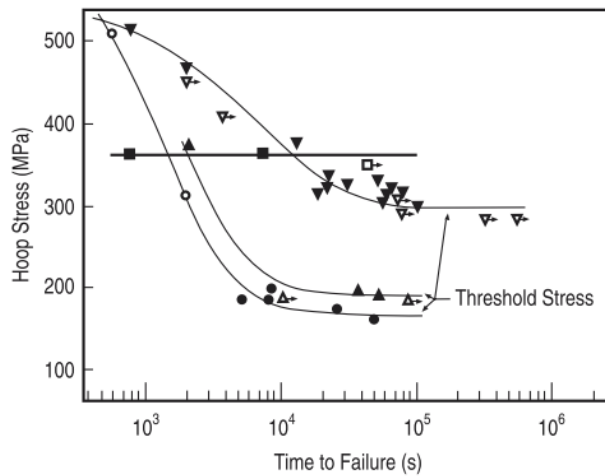


Figure 21
 Effect of hoop stress on time to failure in closed tube tests with an iodine atmosphere [95]

Objective

This subtask aims at obtaining SCC failure data for irradiated cladding tubes for use and implementation in fuel performance codes.

Experimental

Closed tube tests are performed by keeping a closed cladding specimen at a pre-determined internal pressure and temperature until failure. This method yields time-to-failure data. In temperature and stress regions, where creep is important, the data can be used to obtain creep models and criteria for creep failure of the material. By adding Iodine crystals to the specimen tube, time-to-failure data can be obtained for I-SCC failures as a function of stress and temperature. The material used in these tests has to be sensitive to stress corrosion cracking and thus actual irradiated cladding material is preferred. After the test the failure mechanism can be verified by fractography.

In this Subtask it is proposed to make closed tube tests using irradiated cladding samples. Based on modellers’ requirements, a test matrix will be determined at the beginning of SCIP III. Tests will be performed for a range of temperatures and hoop stresses. An example of a test matrix is shown in Table 9.

Table 9

Example of test matrix to generate SCC data

	300°C	350°C	400°C
250 MPa		X	X
350 MPa		X	X
450 MPa	X	X	
550 MPa	X		

The tube samples will be loaded with Iodine, pressurised and sealed by for example welding. The samples are then placed in a pre-heated furnace until failure or for a specified hold time. A few samples will be tested without Iodine as reference. Post-test characterisation will include visual inspection, profilometry, fractography and metallography.

The CDI models typically use the yield stress or mechanical strength to normalise the stress data. Thus, some tensile tests of the material will also be included in the experimental measurements to obtain such properties for normalisation.

Candidate material

The candidate materials for this task are modern BWR and PWR cladding materials, for example BWR Zircaloy-2 cladding with liner. Non-liner material could be tested for comparison with old existing results. For PWRs, the possible candidate materials could be ZIRLO™, M5™ or other similar standard materials of today. Modern fuel materials of both PWR and BWR type are available at Studsvik. Details to be further discussed.

Time schedule

- Year 1: Define the test matrix and identify the materials to be used. Cooperate with the modelling task to optimise the test matrix. Prepare and commission the test equipment. Start sample fabrication.
- Year 2: Continue sample fabrication and perform testing.
- Year 3: Continue testing. Perform post-test examinations and measurements.
- Year 4: Data analysis and reporting. Cooperate with modelling task to compare and evaluate the new CDI dataset compared to existing datasets.

2.3.2 Subtask 3.2 – Chemistry

Main authors: Pia Tejland, Hans-Urs Zwicky

Background

It is a given fact that iodine is an active agent in stress corrosion cracking (SCC) leading to PCI fuel rod failures. Numerous investigations have shown that some metal iodides like those of iron, aluminium, zirconium and tellurium cause SCC just like iodine itself. Gaseous ZrI₄ was found to be the most corrosive agent of all iodides. In laboratory experiments, CsI was also identified as an agent causing SCC under gamma ray irradiation [96].

An issue that is far from having been elucidated is the timing of release of active fission products relative to the mechanical load of the cladding. From ramp tests, it is difficult, if not impossible to gain insight into this

issue; therefore, it has to be investigated by means of laboratory experiments like mandrel tests with equipment that allows controlling the iodine level and its variation with time.

A limited number of mandrel tests have been performed within SCIP III with upgraded equipment that allows controlling the oxygen level in the test atmosphere within very tight limits. The results clearly indicate that oxygen has a mitigating effect on PCI performance, but the database needs to be further extended.

Objectives

The objectives of this subtask are the following:

- Investigate the influence of the timing of iodine ingress relative to the mechanical load on the cladding on PCI performance
- Extend the database on the mitigating effect of oxygen on PCI performance
- Study the impact of other potentially active species on PCI performance

Experimental

Timing of iodine ingress

A series of mandrel tests will be performed with well-defined irradiated cladding material. The point-of-time of iodine ingress relative to the mechanical load evolution is varied. The test series will start with a number of scoping tests that aim at determining potential transition conditions. Based on the results, the test matrix is refined, in order to assess conditions of interest. Overall, at least ten tests will be performed. Depending on budget, the experimental matrix might be extended to more than one type of cladding material.

Impact of oxygen

On the basis of SCIP III data, a matrix of 10-20 mandrel tests will be defined, in order to fill in gaps and to extend the database to additional types of fuel cladding. The scope of the experimental matrix depends on budget and availability of test material of interest.

Impact of other potentially active species

In the order of ten scoping tests will be performed with some selected cladding materials, varying the type and amount of the potentially active species. The detailed definition of the experimental matrix will require negotiations between SCIP participants, experts and Studsvik, taking into account the status of knowledge on the one hand and possibilities and limitations for experiments in the upgraded mandrel test equipment on the other hand.

2.3.3 Subtask 3.3 – Microstructure and microchemistry

Main authors: Pia Tejlund, Hans-Urs Zwicky

Background

As mentioned above, it is a given fact that iodine is an active agent in stress corrosion cracking (SCC) leading to PCI fuel rod failures. It has also been demonstrated that other species, e.g. some metal iodides, cause SCC. However, mode of action of the active species, their way to and their distribution at the location of concern, their chemical and physical form and many other aspects are still not well understood. In order to make the next step towards detailed understanding of the SCC mechanism, another class of equipment than the one Studsvik has at its disposal will be necessary. This has been demonstrated in collaboration between SCIP III and PACE [97].

Whereas Studsvik disposes of a large amount of sample material with PCI cracks, e.g. from mandrel tests, from ramp experiments and from fuel rods that had failed during reactor operation, potential partners like the University of Manchester are operating instruments for advanced characterisation of stress corrosion cracks. Examples of such techniques are SEM and optical imaging, X-ray tomography and serial sectioning to determine crack morphology, SEM and TEM EDX and NanoSIMS for chemical analysis of very small areas, and Transmission Kikuchi diffraction, 3D and 2D EBSD and diffraction contrast tomography for orientation analysis.

SCIP III collaboration with PACE led to promising results. A TEM sample containing a crack tip was extracted from a mandrel test sample at Studsvik by means of SEM and a focused ion beam (FIB) (Figure 22) and sent to the University of Manchester for thinning and further characterisation. Elemental distributions were determined in the crack tip region by means of scanning transmission electron microscopy (STEM) combined with EDX. Nanoscale secondary ion mass spectrometry (nanoSIMS) confirmed the distribution of iodine determined by EDX and indicated that iodine ... (*SCIP III proprietary information deleted*) (Figure 23). This might have been observed for the first time ever.

Within this subtask, microstructure and microchemistry inside cracks and at the crack tip of irradiated cladding samples that had experienced SCC will be investigated by means of TEM, nanoSIMS and other techniques in collaboration with external partners, e.g. University of Manchester or Swerea KIMAB.

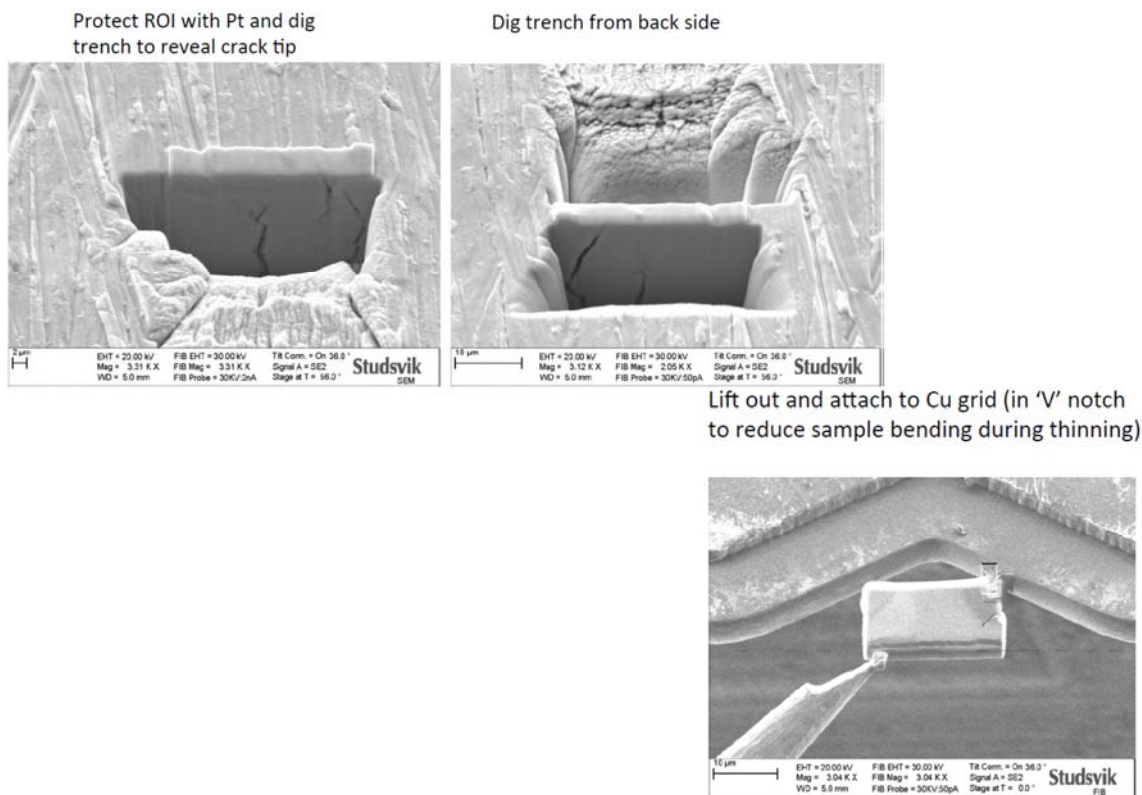


Figure 22
Preparation of TEM sample from mandrel test specimen at Studsvik by means of TEM-FIB [97]

(Figure containing SCIP III proprietary information deleted).

Figure 23
Iodine distribution in the region of a crack tip in a mandrel test sample measured with TEM-EDX (left) and nanoSIMS (right) [97]

Objectives

The subtask aims at supporting the understanding of the SCC mechanism by investigating chemistry and microstructure inside cracks and at crack tips.

Experimental

Candidate materials

Potential material for samples to be prepared for advanced examinations are, amongst others, numerous samples from mandrel tests performed within SCIP III and ramp tested rodlets that had failed by PCI or at least developed incipient stress corrosion cracks.

Preparation of TEM samples

Based on post-test examinations, samples containing SCC tips will be cut out from mandrel and ramp test specimens. TEM samples will be cut out

by means of the Studsvik SEM-FIB equipment and sent to the laboratories of the collaboration partners.

Investigation of microstructure and microchemistry

After sample thinning, microstructure and microchemistry inside the crack and in front of the crack tip will be investigated by means of advanced techniques like STEM-EDX, nanoSIMS and others.

Scope of investigations

The scope of work will be defined later on. It depends on budget limitations availability of equipment for advanced examinations and on availability of suitable material.

2.3.4 Subtask 3.4 – Operational parameters

Main author: Hans-Urs Zwicky

Background

Introducing large producing capacities of wind and photovoltaic power leads to significantly changed demands of grid operators and suppliers of electricity on plants that were originally designed for base-load electricity production, amongst others nuclear power plants. Operation with significantly reduced power over extended periods of time might be necessary. This might well impact operating limits, e.g. PCI rules established on the basis of originally intended operating regimes.

A consequence of extended periods of operation at reduced power is a different inventory of fission products with shorter half-lives in the fuel. In the case of iodine, the inventory of stable ^{127}I and long-lived ^{129}I is not strongly impacted and remains more or less proportional to the burnup. The content of isotopes with shorter half-lives on the other hand, in particular ^{131}I (8.02 d), ^{132}I (2.3 h), ^{133}I (20.8 h) and ^{135}I (6.61 h) is proportional to power, which means that less active agent might be released in the case of a transient after an extended period of reduced power operation. This could well lead to a different timing of iodine ingress and to a lower amount of active agent in the region of crack tips, compared to a comparable transient at full power operation.

The parameter study on the timing of iodine ingress in Subtask 3.2 – Chemistry will hopefully reveal some correlations between transient parameters, availability of active agent and susceptibility to SCC. This subtask will verify these findings by means of a limited number of ramp tests.

Objectives

The objective of this subtask is to verify correlations between transient parameters, availability of active agent and susceptibility to PCI.

Experimental

Ramp tests

2-4 ramp tests will be performed in the Halden ramp test rig. The tested rodlets should stem from non-liner fuel rods with intermediate burnup level. The inventory of SCC active agents is controlled by an extended period of conditioning (several months) at low power. Planning of the tests will be supported by modelling.

The scope of the tests depends on available budget, on the costs of the ramp tests and of pre- and post-test characterisations and on the availability of suitable test material.

Pre- and post-test examinations

The father rods of the ramp test rodlets are characterised by detailed post-irradiation examinations, including visual inspection, profilometry, oxide thickness measurements, gamma scanning, puncturing and fission gas release analysis, and light optical microscopy (metallography, ceramography). At least in one of the cases, the fuel pellet is characterised by advanced examination methods, e.g. SEM-WDS and LA-ICP-MS.

After the ramp tests, the rodlets are examined in the same way as the father rod, including fission gas release analysis, if the tested rodlet did not fail.

Modelling

In addition to base irradiation and ramp test modelling, the inventory of potentially active agents is established by means of suitable codes.

2.4 Task 4 – Modelling

Main author: Joakim Karlsson

2.4.1 Background

The reliable prediction of fuel rod behaviour in nuclear power reactors constitutes a basic demand for safety-based calculations, for design purposes and for fuel performance assessments. There are many nuclear fuel performance codes, some of which are available in public domain, though most of them are developed and used by vendors, utilities or authorities.

Generally, two types of fuel performance codes are being applied, corresponding to normal operation and to design basis accident conditions, respectively. A reliable prediction of fuel rod performance is important for fuel rod design and safety evaluation in nuclear power reactors. More realistic predictions of fuel performance allow improved safety, operating margins and economics as well as potentially higher fuel management flexibility.

Most codes were initiated in the 1960ies and have undergone continuous improvement up to now. The trend is to have codes with more and more realistic and mechanistic models based on an understanding of the underlying physics, and striving to avoid pure empirical correlations. It is thus of outmost importance to better understand fuel behaviour, not merely to observe relations but to understand the nature of what is going on. The improved understanding should be implemented into the codes, thus facilitating code development based on mechanistic, physical and chemical reactions at micro-level. Modelling the physics and chemistry at micro-level is one way to reduce the risk for unreliable code predictions, when the modelled operating conditions and material conditions are outside the experience base of observations.

The fuel fragmentation behaviour which has been observed in Studsvik and Halden LOCA tests clearly represents cases, where the existing fuel performance models could not predict what occurred. The nuclear community agrees that there are most likely many potential combinations of circumstances outside the experience base which may very well give surprising results not yet predicted in the standard models.

SCIP presents an environment, where authorities, vendors and utilities are all participating in the meetings, discussing the same results. The SCIP project can thus facilitate a mutual understanding and support code benchmarking, verification, development and more fundamental discussions about the underpinning fundamentals of the actual fuel behaviour.

Originally the SCIP I and II programs did not include an integrated modelling effort. However, SCIP I members expressed a need to connect experiments to theoretical modelling, since modelling is the standard tool used to assess fuel behaviour in operation and transient conditions. Thus, SCIP I organized two separate modelling workshop (MWS) events in Studsvik in 2007 [98] and in Cologne, Germany in 2008 [99]. In SCIP II, a larger MWS effort was made with contributions presented at three consecutive SCIP meetings [100]. The main MWS meeting took place in Cordoba, Spain in November 2012. All three workshops in SCIP I and II focused on the modelling of reactor ramp tests. In SCIP III, however, the workshop has been part of the Task 3 deliverables and focused on modelling of base irradiation and semi-integral LOCA tests.

2.4.2 Modelling in SCIP IV

Modelling in SCIP IV will be an integrated part of the project and will be planned and managed by Studsvik. The modelling efforts will consist of in-kind and voluntary contributions. All contributions are welcome and the aim is to include modelling performed by several different organisations using different code systems. A diversity of models and methods is deemed useful when studying new phenomena and it will encourage model development. It is expected that a few modelling partner teams will continuously follow and perform modelling in parallel with the experimental program with regular updates at the SCIP meetings. This will

be a planned and integrated part of SCIP. The integrated modelling will support experiment planning before tests and interpretation and evaluation after tests.

Furthermore, voluntary modelling contributions are very much encouraged and these contributions may model any tests or cases and present results at any SCIP meeting. The broadest possible participation is encouraged to get a broad and rewarding discussion in place.

SCIP IV shall not by itself develop any codes or parts of codes, but focus on supporting the participants' code development. The experimental tasks will provide input to the modelling in Task 4 by providing a large amount of high quality data. With the support of the participants, improved understanding of the actual mechanistic, physical and chemical processes in the fuel under different scenarios will be achieved. Modelling shall, in addition to being a part of the analysis, also be utilised to plan experiments, integral as well as separate effect tests.

The fuel fragmentation phenomenon is a typical example of results not predicted or expected from modelling, thus a dual approach is planned. There shall be tests to explore the behaviour outside the experience band and tests to confirm experience. These results may be used in the code development in the participant organisations. As stated above, modelling predictions will also be used to plan and give input to experiments, supporting separate effect studies as well as integral experiments.

The modelling workshops in SCIP have been highly appreciated and it is proposed to continue these efforts in SCIP IV. The workshop provides a concerted and focused effort to facilitate code benchmarking and development work among the SCIP participants. The workshop will be based on a well-defined and limited set of interesting modelling cases drawing on the experimental data achieved in the SCIP program.

Objective

Support SCIP IV with pre- and post-test modelling calculations of tests and experiments using different codes and models. More specifically, the objectives are to:

- Provide input to the design of test matrices and selection of test parameters
- Improve evaluation/interpretation of the results
- Extend the basis for the validation of existing models and identify model improvements and the data needs for such improvements

Procedure

SCIP IV shall ensure that modelling is performed within the project and shall plan and manage the workshop(s). SCIP members will be invited to participate as modelling partners using the codes of their choice. The project shall compile data sets to be used by the modellers.

Deliverables

The basic deliverable is support and input to all experimental tasks in SCIP IV. The work in the modelling task will also result in several reports on the modelling results achieved including comparisons to experimental data. A workshop will be organized with benchmark comparisons of results from participating codes for the same test cases.

3 Conclusions

Like the earlier projects, SCIP IV is planned to be a five-year program with an overall budget in the order of 14 M€ (SCIP III fee +10 %), starting in July 2019. It will be organised in a similar way as SCIP III. The present report describes potential Tasks and Subtasks of SCIP IV as a basis for discussions within potential participants' organisations.

In total, 19 Subtasks are described in the present proposal. Eight Subtasks within Task 1 aim at studying fuel and cladding performance issues related to interim storage. The seven Subtasks described under Task 2 represent a continuation and extension of work performed in SCIP III to investigate LOCA issues. Even Task 3 is a continuation and extension of work performed in SCIP III related to PCI. As in SCIP III, modelling efforts supporting planning and interpretation of experiments in Tasks 1 – 3 will be concentrated in a dedicated Task.

Performing all described tasks would exceed by far the SCIP IV budget. Therefore, the interaction with potential participants is supposed to provide a prioritisation that will allow defining the final scope of work within the disposable resources.

Whatever the result of the prioritisation exercise will be, SCIP IV will constitute another one in a row of successful collaborative projects adding valuable results to the knowledge base in the field of fuel and cladding performance.

4 References

- [1] M. Quecedo, M. Lloret, J.M. Conde, C. Alejano, J.A. Gago and F.J. Fernandez
Results of thermal creep tests on highly irradiated Zirlo
Nuclear Engineering and Technology, Vol. 41 No. 2,
March 2009
- [2] Per Magnusson
xxx
Ph D thesis xxx
- [3] Hyun-Gil Kim, Yong-Hwan Jeong and Kyu-Tae Kim
The effects of creep and hydride on spent fuel integrity during interim dry storage
Nuclear Engineering and Technology, Vol. 42 No. 3,
June 2010
- [4] C. Cappelaere, R. Limon, D. Gilbon, T. Bredel, O. Rabouille, P. Bouffieux and J. P. Mardon
Impact of irradiation defects annealing on long-term thermal creep of irradiated Zircaloy-4 cladding tube
Zirconium in the Nuclear Industry: Thirteenth International Symposium, ASTM STP 1423, G. D. Moan and P. Rudling, Eds., ASTM International, West Conshohocken, PA, 2002, pp. 720-739
- [5] J.R. Santisteban, M.A. Vicente-Alvarez, P. Vizcaíno, A.D. Banchik and J.D. Almer
Hydride precipitation and stresses in zircaloy-4 observed by synchrotron X-ray diffraction
Acta Materialia 58 (2010) 6609-6618
- [6] E. Krempl
Creep-plasticity interaction
in Creep and Damage in Materials and Structures, edited by Holm Altenbach and Jacek J. Skrzypek, Springer-Verlag Wien 1999, pp. 285-336.
- [7] U.S.NRC
Cladding considerations for the transport and storage of spent fuel
SFST-ISG-11, Revision 3, Nov. 2003
- [8] Chantal Cappelaere, Roger Limon, Christelle Duguay, Gérard Pinte, Michel Le Breton, Pol Bouffieux, Valérie Chabretou and Alain Miquet
Thermal creep model for CWSR Zircaloy-4 cladding taking into account the annealing of the irradiation hardening
Nuclear Technology 177:2 (2012) 257-272, DOI: 10.13182/NT12-A13370

- [9] *Management of Damaged Spent Nuclear Fuel*
IAEA Nuclear Energy series report No. NF-T-3.6
ISBN 978-92-0-103809-8, 2009
- [10] Jongwon Choi, Young-Chul Choi and Dong-Hak Kook
Integrity Study of Spent PWR Fuel under Dry Storage Conditions-14236
WM2014 Conference, March 2-6, 2014, Phoenix, Arizona, USA
- [11] Hyun-Gil Kim and Yong Hwan Jeong
The effects of creep and hydride on spent fuel integrity during dry storage
Nuclear Engineering and Technology, Vol. 42 No. 3 June 2010
- [12] Ken B. Sorenson and Brady Hanson
Making the case for safe storage of used nuclear fuel for extended periods of time: combining near-term experiments and analyses with longer-term confirmatory demonstrations
Nuclear Engineering and Technology, Vol. 45 No. 4 August 2013
- [13] Felix Boldt and Maik Stuke
Studsvik Cladding Integrity Project – GRS Suggestions for Phase IV
GRS, 8 September 2017
- [14] W.L. Mudge
Effect of hydrogen on the embrittlement of zirconium and zirconium-tin alloys
Symposium on Zirconium and Zirconium alloys, xxx, Metals Park, OH, 146-167 (1953)
- [15] C.E. Coleman and D.Hardie
The hydrogen embrittlement of zirconium in slow-bend tests
Journal of Nuclear Materials, **19**(1),1-8 (1966)
- [16] J.B. Bai, C. Prioul and D.Francois
Hydride embrittlement in Zircaloy-4 plate: Part I, Influence of microstructure on the hydride embrittlement in Zircaloy-4 at 20°C and 350°C
Metallurgical Transactions, **25A**, 1185-1197 (1994)
- [17] D. Hardie
The influence of the matrix on the hydrogen embrittlement of zirconium in bend tests
Journal of Nuclear Materials, **42**(3), 317-324 (1972)
- [18] S. Sagat and M.P. Puls
xxx
SMiRT 17, paper # G06-4

- [19] A. McMinn, E.C. Darby and J.S. Schofield
The terminal solid solubility of hydrogen in zirconium alloys
Twelfth International Symposium of Zirconium in the Nuclear Industry, Editors: G.P. Sabol and G.D. Moan.
ASTM STP 1354, p.173-195 (2000)
- [20] P. Vizaino, A.D. Banchik and J.P. Abriata
Solubility of hydrogen in Zircaloy-4: irradiation induced increase and thermal recovery
Journal of Nuclear Materials, 304:96-106 (2002)
- [21] J.J. Kearns
Terminal solubility and partitioning of hydrogen in the alpha phase of zirconium, Zircaloy-2 and Zircaloy-4
Journal of Nuclear Materials, 22:292-303 (1967)
- [22] V. Grigoriev
Parametric study of DHC in fuel cladding
Workshop on hydrogen induced failures, Nov. 17, Sweden (2009)
- [23] Y.S. Kim
Delayed hydride cracking of spent fuel rods in dry storage
Journal of Nuclear Materials 378, p 30-34 (2008)
- [24] C.E. Coleman
The CANDU experience AECL, History: Cause and remedies xxx
Workshop on hydrogen induced failures, Nov. 17 2009, Sweden
- [25] V. Grigoriev and R. Jakobsson
Delayed hydrogen cracking velocity and J-integral measurements on irradiated BWR cladding
Journal of ASTM International, 2(8), September 2005
- [26] F.H. Huang and W.J. Mills
Delayed hydride cracking behavior for zircaloy-2 tubing
Metallurgical Transaction A, 22A:2049-2060 (1991)
- [27] Y.S. Kim, S.C. Kwon and S.S. Kim
Crack growth pattern and threshold stress intensity factor, K_{IH} , of Zr-2.5% Nb alloy with the notch direction
Journal of Nuclear Materials, 280:304-311 (2000)
- [28] D. Yan and R.L. Eadie
The threshold behaviour of delayed hydride cracking in Zr-2.5wt%Nb
International Journal of Pressure Vessels and Piping, 77:167-177 (2000)

- [29] S-Q. Shi and M.P. Puls
Criteria for fracture initiation at hydrides in zirconium alloys, I: sharp crack tip
Journal of Nuclear Materials, 208:232-242 (1994)
- [30] C.E. Coleman and J.F.R. Ambler
Susceptibility of zirconium alloys to delayed hydride cracking
Zirconium in the Nuclear Industry, ASTM STP 633, p. 589-607, Editors: A.L. Lowe and G.W. Parry (1977)
- [31] T. Kubo, K. Sakamoto and T. Higuchi
Development of a New Technique for the In-situ Observation Of the DHC Process under a SEM to Measure the Crack Extension Rate in a Radial Direction of Zry-2 Tubes
2008 Water Reactor Fuel Performance Meeting, October 19-23 in Seoul, Korea, (2008)
- [32] International Atomic Energy Agency
Evaluation of conditions for hydrogen induced degradation of Zirconium alloys during fuel operation and storage
IAEA-TECDOC-1781
- [33] C.F. Tiffany, J.N. Masters
Applied fracture mechanics
Fracture Toughness Testing and its Applications
ASTM STP 381, W.F. Brown, Jr., Ed., American Society for Testing and Materials, Philadelphia, PA., 1965, pp. 249-277
- [34] US Nuclear Regulatory Commission
Standard Review Plan for Spent Fuel Dry Storage Systems at a General License Facility
NUREG-1536, 2009
- [35] E.W. Brach
Cladding Consideration for the Transportation and Storage of Spent Fuel
U.S.NRC Interim Staff Guidance – 11, Revision 3,
Spent Fuel Project Office, 2003
- [36] P. Efsing, K. Pettersson
Delayed Hydride Cracking in Irradiated Zircaloy Cladding
Zirconium in the Nuclear Industry – Twelfth International Symposium, ASTM STP 1354, G.P. Sabol and G. D. Moan, Eds., American Society for Testing and Materials, West Conshohocken, PA., 2000, pp. 340-355.

- [37] Jy-An Wang and Hong Wang
Mechanical Fatigue Testing of High-Burnup Fuel for Transportation Applications
NUREG/CR-7198, ORNL/TM-2014/214 (2015)
- [38] Viktor Ballheimer, Frank Wille and Bernhard Droste
Mechanical Safety Analysis for High Burn-up Spent Fuel Assemblies under Accident Transport Conditions
PATRAM (2010)
- [39] P. C. Purcell and M. Dallongeville
Testing of LWR Fuel Rods to Support Criticality Safety Analysis of Transport Accident Conditions
RAMTRANS Vol.15, Nos. 3–4, pp.163–164 (2004)
- [40] M. Dallongeville, J. Werle and G. McCreesh
Fuel Integrity Project: Analysis of Results of Tests on Light Water Reactor Fuel Rods
RAMTRANS Vol.16, No.2, pp.125-133 (2005)
- [41] D. Papaioannou, R. Nasyrow, V.V. Rondinella, W. Goll, H.-P. Winkler, R. Liedtke, D. Hoffmann
xxx
Proc. KTG 2009, May 12-14, 2009, Dresden, Germany.
- [42] V.V. Rondinella, T. Wiss, D. Papaioannou, R. Nasyrow, F. Cappia, S. Van Winckel, D. Serrano-Purroy, D. Wegen
Spent Nuclear Fuel in View of Long-Term Storage
IHLRWM 2015, Charleston, SC, April 12-16, 2015
- [43] R. A. Lorenz et al.
Fission Product Release from Highly Irradiated LWR Fuel
NUREG/CR-0722. ORNL/NUREG/TM-287/R1 (1980)
- [44] R. E. Einziger and C. Beyer
Characteristics and Behavior of High-Burnup Fuel that May Affect the Source Terms for Cask Accidents
Nuc. Tech. Vol. 159, pp. 134 (2007)
- [45] P. Askeljung, J. Flygare and J Martinsson
NRC LOCA testing program at Studsvik, results on high burnup fuel
2011 Water Reactor Fuel Performance Meeting, Chengdu, China, September 11-14, 2011, paper T3-039.
- [46] G. Bjorkman
The Buckling of Fuel Rods in Transportation Casks Under Hypothetical Accident Conditions
14th International Symposium on the Packaging and Transportation of Radioactive Materials (PATRAM 2004), Berlin, Germany, September 20-24, 2004.

- [47] *Krav på behållare för slutförvaring av läckande bränslestavar*
SKB Report 1495782 Version 2.0, 2015
- [48] H. Jung, et al.
Extended Storage and Transportation: Evaluation of Drying Adequacy
xxx 2013
- [49] USNRC. xxx
- [50] *Standard Guide for Drying Behavior of Spent Nuclear Fuel*
ASTM C1553 xxx
- [51] D. Jäternäs, P. Tejländ
Advanced PIE on R2D5 and 3V5/Q13
SCIP III Program Review Group Meeting, May 2017
- [52] A. Puranen, D. Jäternäs, P. Tejländ, J. Karlsson
Advanced PIE on R2D5 and 3V5/Q13 New SEM and LA-ICP-MS Xe results
SCIP III Program Review Group Meeting, October 2016
- [53] O Tengstrand
Advanced PIE status report
SCIP III Program Review Group Meeting, May 2017
- [54] J.C. Killeen
Fission gas release and swelling in UO₂ doped with Cr₂O₃
J. Nucl. Mat. **88** (1980) 177 – 184
- [55] C. Delafoy, V.I. Arimescu, R.M. Hengstler-Eger,
H. Landskron, A. Moeckel, P. Bellanger
AREVA Cr₂O₃-doped fuel: increase in operational flexibility and licensing margins
TopFuel Reactor Fuel Performance 2015, 13-27 September 2015, Zürich, Switzerland.
- [56] J. Arborelius, K. Backman, L. Hallstadius, M. Limbäck,
J. Nilsson, B. Rebensdorff, G. Zhou, K. Kitano,
R. Löfström, G. Rönnberg
Advanced doped UO₂ pellets in LWR applications
Journal of Nuclear Science and Technology **43** (2006) 967 – 976
- [57] J.H. Davies, S. Vaidyanathan, R.A. Rand
Modified fuel for high burn-up
Proceedings of the TopFuel '99 Conference, SFEN/ENS,
pp 385-395

- [58] P. Garcia, A. Bouloré, Y. Guérin, M. Trotabas, P. Goeuriot
In-pile densification of MOX fuels in relation to their initial microstructure
ANS International Topical Meeting on Light Water Reactor Fuel Performance, April 10-13, 2000, Park City, Utah
- [59] Y. Guérin, J. Noirot, D. Lespiaux, C. Struzik, P. Garcia, P. Blanpain, G. Chaigne
Microstructure evolution and in-reactor behaviour of MOX fuel
ANS International Topical Meeting on Light Water Reactor Fuel Performance, April 10-13, 2000, Park City, Utah
- [60] J. Karlsson et al.
SCIP III – Test Method Descriptions
STUDSVIK/N-15/315, STUDSVIK-SCIP-III-196
- [61] M. Flanagan, P. Askeljung, A. Puranen, *Post-Test Examination Results from Integral, High-Burnup, Fueled LOCA Tests at Studsvik Nuclear Laboratory*, United States Nuclear Regulatory Commission, Office of Nuclear Regulatory Research, NUREG-2160, August 2013
- [62] F. Nisserud Nazary
SCIP III LOCA design report
STUDSVIK/N-15/341, STUDSVIK-SCIP III-197
- [63] P. Magnusson
LOCA qualification report – Qualification of a new integral LOCA test device for the SCIP III program
STUDSVIK/N-16/009
- [64] P. Magnusson, D. Minghetti
LOCA test to study the effect of heating rate
SCIP III Program Review Group Meeting, June 2016
- [65] J. Karlsson, A. Puranen, P. Magnusson, M. Lundström
Heating tests for investigation of temperature ramp rate and temperature threshold
SCIP III Program Review Group Meeting, June 2016
- [66] P. Magnusson, J. Karlsson, A. Puranen, P. Tejland, D. Minghetti, M. Lundström, P. Beccau
Strain threshold, burst and depressurization
SCIP III Program Review Group Meeting, May 2017
- [67] A. Puranen, D. Minghetti
Status of heating tests
SCIP III Program Review Group Meeting, January 2015

- [68] O. Spieler, B. Kennedy, U. Kueppers, D. B. Dingwell, B. Scheu, J. Taddeucci
The fragmentation threshold of pyroclastic rock
Earth and Planetary Science Letters 226, 2004, 139-148
- [69] A. C. Fowler, B. Scheu, W. T. Lee, M. J. McGuinness
A theoretical model of the explosive fragmentation of vesicular magma
Proceedings of the Royal Society 466, 2010, 731-752
- [70] M. Billone, Y. Yan, T. Burtseva, R. Daum
Cladding embrittlement during postulated loss-of-coolant accidents
NUREG/CT-6967, ANL-07/04, 2008
- [71] L. Baker, L.C. Just
Studies of water-metal reactions at high temperatures III. Experimental and theoretical studies of zirconium water reactions
Technical Report ANL-6548, Argonne National Laboratory, Argonne, IL, USA, 1962
- [72] J.V. Cathcart, R.E. Pawel, R.A. McKee et al.
Zirconium metal-water oxidation kinetics: IV. Reaction rate studies
Technical report ORNL/NUREG-17, Oak Ridge National Laboratory, TN, USA, 1977
- [73] G. Schanz
Recommendation and supporting information on the choice of zirconium oxidation models in severe accident codes
Forschungszentrum Karlsruhe Report, FZKA 6827, Karlsruhe, Germany, 2003
- [74] F. Nagase, T. Otomo, H. Uetsuka
Oxidation kinetics of low-Sn Zircaloy-4 at the temperature range from 773 to 1573 K
J. Nucl. Sci. Technol. 40, 213-219, 2003
- [75] S. Leistikow, G. Schanz
Oxidation kinetics and related phenomena of Zircaloy-4 fuel cladding exposed to high temperature steam and hydrogen-steam mixtures under PWR accident conditions
Nucl. Engin. & Design 103, 65-84, 1987
- [76] S. Kawasaki, T. Furuta, M. Suzuki
Oxidation of Zircaloy-4 under high temperature steam atmosphere and its effect on ductility of cladding
J. Nucl. Sci. Technol. 15, 589-596, 1978

- [77] M. Le Saux, et al.
Influence of Pre-Transient Oxide on LOCA High Temperature Steam Oxidation and Post-Quench Mechanical Properties of Zircaloy-4 and M5™ cladding
Proceedings of the 2011 Water Reactor Fuel Performance Meeting, Chengdu, China, September 11-14, 2011
- [78] I.L. Bramwell, T.J. Haste, D. Worswick, P.D. Parsons
An experimental investigation into the oxidation of Zircaloy-4 at elevated pressures in the 750 to 1000°C temperature range
Zirconium in the Nuclear Industry, 10th International Symposium, Garde, A. M., Bradley, E. R. (Eds)
ASTM STP 1245, American Society for Testing and Materials, Philadelphia, PA, USA, 450-465, 1994
- [79] K. Park, K. Kim, J. Whang
Pressure effects on high temperature Zircaloy-4 oxidation in steam
ANS Topical Meeting on Light Water Reactor Fuel Performance, Park City, Utah, April 10-13, 2000
- [80] G. Hache, H.M. Chung
The history of LOCA embrittlement criteria
Proc. OECD meeting on LOCA Fuel Safety Criteria
Aix-en-Provence, France, March 22-23, 2001,
NEA/CSNI/R (2001) 18
- [81] *OECD, CSNI technical opinion paper No 13- LOCA criteria basis and test methodologies*
OECD Nuclear Energy Agency, 2011
Report NEA/CSNI/R(2011)/7
- [82] R. Kennedy, J. Nie, C. Hofmayer
Evaluation of JNES Equipment Fragility Tests for USE in Seismic Probabilistic Risk Assessments for U.S. Nuclear Power Plants
NRC NUREG CR/7040, 2011
- [83] M.C. Billone
Assessment of Current Test Methods for Post-LOCA cladding Behaviour
NRC NUREG/CR-7139, NAL-11/52, 2011
- [84] M. Yamato, F. Nagase, M. Amaya
Evaluation of fracture resistance of ruptured, oxidized, and quenched Zircaloy cladding by four-point-bend tests
Journal of Nuclear Science and Technology, 2014, Vol 51, No. 9, 1125-1132

- [85] M. Flanagan
Mechanical Behavior of Ballooned and Ruptured Cladding
United States Nuclear Regulatory Commission, Office of
Nuclear Regulatory Research
NUREG-2119, February 2012
- [86] K. Une, S. Kashibe, A. Takagi
*Fission Gas Release Behavior from High Burnup UO₂ fuels
under Rapid Heating Conditions*
Journal of Nuclear Science and Technology, Volume 43,
1161-1171, (2006)
- [87] Pontillon, Y., Ferroud-Plattet, M.P., Parrat, D., Ravel, S.,
Ducros, G., Struzik, C., Aubrun, I., Eminet, G.,
Lamontagne, J., Noirot, J., and Harrer, A.
*Experimental and Theoretical Investigation of Fission Gas
Release from UO₂ up to 70 GWd/t under Simulated LOCA
type conditions: The GASPARD Program*
Top Fuel 2004, Orlando, USA, September 19-22, 2004,
paper 1025, (2004)
- [88] Marcet, M., Pontillon, Y., Desgranges, L., Noirot, J.,
Lamontagne, J., Aubrun, I., Pasquet, B., Valot, Ch.,
Cognon, H., and Blanpain, P.
*Contribution of high burnup-up structure to fission gas
release under transient conditions*
Top Fuel 2009, Paris, France, September 14-17, 2009
paper 2055, (2009)
- [89] Bianco, A., Vitanza, C., Seidl, M., Wensauer, A., Faber,
W., and Maciám, R.
*Experimental investigation on the causes for pellet
fragmentation under LOCA conditions*
Journal of Nuclear Materials, Volume 465, p. 260-267,
(2015)
- [90] Per Magnusson, Carl Adamsson, Daniel Jädernäs, Gunnar
Rönnerberg, David Schrire, Anna Alvestav, and Marcus Seidl
A study of transient FGR by integral LOCA tests
WRFPM meeting 2016, paper 17070, Boise, USA, 2016
- [91] C. Anghel, H.U. Zwicky,
*Summary of the Pellet-Cladding Interaction (PCI) seminar
organised in Studsvik, 31st May – 1st June 2010*
Studsvik Report N-10/169, STUDSVIK-SCIP II-107, 2010-
10-08

- [92] H.U. Zwicky
Workshop on Fuel Rod Behaviour Modelling, 3rd SCIP Ramp Test Benchmark, November 15, 2011, Córdoba, Spain
Studsvik Technical Note N-12/027, STUDSVIK-SCIP II-136, 2012-01-31
- [93] H.U. Zwicky, I. Arimescu
Workshop on Fuel Rod Behaviour Modelling, 3rd SCIP Ramp Test Benchmark – Part 2 (June 12, 2012) and Part 3 (November 13, 2012), Studsvik, Sweden
Studsvik Technical Note N-13/101, STUDSVIK-SCIP II-155, 2013-03-05
- [94] W. Lyon et al.
PCI Analysis and Fuel Rod Failure Prediction using FALCON
Proceedings of Top Fuel 2009, Paris, France
- [95] D. Cubicciotti, R.L. Jones, and B.C. Syrett
Stress Corrosion Cracking of Zircalloys
EPRI NP-1329 (March 1980)
- [96] *Review of fuel failures in water cooled reactors*
IAEA Nuclear Energy Series No. NF-T-2.1, 2010
- [97] Alistair Garner
Advanced characterisation of iodine-induced stress corrosion cracks in Zr alloys
Presentation at SCIP III PRG meeting
28-30 November 2017, Studsvik
- [98] L.E. Herranz et al.
Insights Into Fuel Rod Performance Codes during Ramps: Results of a Code Benchmark based on the SCIP Project Topfuel 2009
- [99] L.E. Herranz et al.
Assessment of fuel rod performance codes under ramp scenarios investigated within the SCIP project
Nucl. Eng Des. 2011
- [100] I Arimescu et al.
Third SCIP Modeling Workshop: Beneficial Impact of Slow Power Ramp on PCI Performance
WRFPM 2014, Sendai, Japan

Abbreviations, Acronyms

ADOPT	Advanced DOped Pellet Technology
ADU	Ammonium diuranate
AOO	Anticipated operational occurrence
AUC	Ammonium uranocarbonate
BJ	Baker-Just (correlation to calculate ECR)
BNFL	British Nuclear Fuels Ltd
BSE	Backscattered electron
BWR	Boiling water reactor
CDI	Cumulative damage index
CFR	Code of federal regulation
CILC	Crud-induced localised corrosion
CIRFT	Cyclic integrated reversible-bending fatigue tester
CP	Cathcart-Pawel (correlation to calculate ECR)
CRP	Coordinated research project
CSED	Critical strain energy density
C _{TSSD}	Terminal solubility limit for hydride dissolution
C _{TSSP}	Terminal solubility limit for hydride precipitation
DBA	Design basis accident
DBTT	ductile-to-brittle transition temperature
DC	Direct current
DCPD	Direct current potential drop
DHC	Delayed hydride cracking
DNB	Departure from nucleate boiling
E110	Russian PWR cladding material
EBSD	Electron backscatter diffraction
EC	Eddy-current (defect testing and oxide layer measurement)
ECCS	Emergency core cooling system
ECR	Equivalent cladding reacted
EDC	Expansion-due-to-compression
EDS	Energy dispersive (X-ray) spectroscopy
EDX	Energy dispersive X-ray spectroscopy
EPMA	Electron probe microanalysis
EPRI	Electrical Power Research Institute
FEG	Field emission gun
FEM	Finite element method
FFRD	Fuel fragmentation, relocation and dispersal
FG	Fission gas
FGR	Fission gas release
FIB	Focused ion beam
GIS	Gas injection system
GNF	Global Nuclear Fuel
HE	Hydrogen embrittlement
HiFi™	PWR cladding material developed by NFI
HVE	Hot vacuum extraction (hydrogen analysis)

ICP-MS	Inductively coupled plasma mass spectrometry
IR	Infrared
I-SCC	Iodine-induced stress corrosion cracking
ITU	Institute for Transuranium Elements
JAEA	Japan Atomic Energy Agency
K_{IH}	Threshold stress intensity factor for DHC ($\text{MPa}\sqrt{\text{m}}$)
LA	Laser ablation
LOCA	Loss-of-coolant accident
LOM	Light optical microscopy
LVDT	Linear Variable Differential Transformer
M5™	AREVA PWR cladding and assembly structural material
MBT	Modified burst test
MIMAS	Micronised MASTer blend
MOX	Mixed uranium-plutonium oxide fuel
MWS	Modelling workshop
NEA	Nuclear Energy Agency
NFI	Nuclear Fuels Industry (Japan)
OECD	Organisation for Economic Co-operation and Development
Optimized ZIRLO™	Westinghouse cladding material
ORIGEN	Code package for calculating nuclide formation and depletion during reactor operation of nuclear fuel
ORNL	Oak Ridge National Laboratory
PACE	Pellet Assisted Cladding dEgradation (international collaboration)
PCI	Pellet-cladding interaction (stress corrosion cracking)
PCMI	Pellet-cladding mechanical interaction
PCT	Peak cladding temperature
PIE	Post-irradiation examination
PLT	Pin-loading tension
POD	Post-oxidation ductility
PQD	Post-quench ductility
PWR	Pressurised water reactor
RCT	Ring compression test
RIA	Reactivity initiated accident
RXA	Recrystallized
SCC	Stress corrosion cracking
SCIP	Studsvik Cladding Integrity Project
SE	Secondary electron
SED	Strain energy density
SEM	Scanning electron microscopy
SFP	Spent fuel pool
SIMS	Secondary ion mass spectrometry
SNF	Spent nuclear fuel
SRA	Stress relieved annealed
STEM	Scanning Transmission Electron Microscopy

TEM	Transmission electron microscopy
TFGR	Transient fission gas release
TNI	...
U.S.NRC	United States Nuclear Regulatory Commission
WDS	Wavelength dispersive (X-ray) spectroscopy
XRD	X-ray diffraction
ZIRLO™	Westinghouse cladding and assembly structural material
ZIRON™	Advanced BWR cladding material (GNF)